IEEE Access
Multidisciplinary | Rapid Review | Open Access Journal

Received April 2, 2019, accepted April 18, 2019, date of publication April 23, 2019, date of current version April 30, 2019.

Digital Object Identifier 10.1109/ACCESS.2019.2912643

Applications of Novel Hybrid Bat Algorithm With Constrained Pareto Fuzzy Dominant Rule on Multi-Objective Optimal Power Flow Problems

GONGGUI CHEN[1,2], JIE QIAN[1,2], ZHIZHONG ZHANG[3], AND ZHI SUN[4]

[1]Key Laboratory of Network Control and Intelligent Instrument, Chongqing University of Posts and Telecommunications, Ministry of Education, Chongqing 400065, China
[2]Chongqing Key Laboratory of Complex Systems and Bionic Control, Chongqing University of Posts and Telecommunications, Chongqing 400065, China
[3]Key Laboratory of Communication Network and Testing Technology, Chongqing University of Posts and Telecommunications, Chongqing 400065, China
[4]Chn Energy Enshi Hydropower Co., Ltd., Enshi 445000, China

Corresponding author: Zhizhong Zhang (zhangzztx@163.com)

This work was supported in part by the Innovation Team Program of the Chongqing Education Committee under Grant CXTDX201601019, in part by the Chongqing University Innovation Team under Grant KJTD201312, and in part by the National Natural Science Foundation of China under Grant 51207064 and Grant 61463014.

ABSTRACT To overcome the premature-convergence of standard bat algorithm in solving the multi-objective optimal power flow (MOOPF) problems, a novel hybrid bat algorithm (NHBA) is proposed in this paper. The suggested NHBA algorithm modifies the local search manner by a monotone random filling model based on extreme (MRFME) and improves the population-diversity by mutation and crossover mechanisms. To obtain the uniformly distributed Pareto optimal set (POS) with zero constraint-violation, an innovative non-dominated sorting method combined with the constrained Pareto fuzzy dominant (CPFD) strategy is put forward in this paper. To verify the superiority of the proposed NHBA-CPFD algorithm, which is federated by the NHBA algorithm and the CPFD strategy, ten MOOPF simulation cases considering the basic fuel cost, the fuel cost with value-point loadings, the total emission, and the active power loss are studied on the IEEE 30-node, IEEE 57-node, and IEEE 118-node systems. In contrast to the NHBA, MOPSO, and NSGA-III algorithms which adopt the constrain-prior Pareto-dominance method (CPM), numerous results validate the NHBA-CPFD algorithm that can achieve more superior compromise solutions and preferable Pareto fronts (PFs) even in the large-scale systems. Furthermore, two performance metrics of generational distance (GD) and hyper-volume (HV) also demonstrate that the NHBA-CPFD algorithm has great advantages to obtain the feasible POS with evenly distribution and favorable-diversity.

INDEX TERMS Novel hybrid bat algorithm, multi-objective optimal power flow problem, constrained Pareto fuzzy dominant strategy, monotone random filling model based on extreme, performance metrics.

I. INTRODUCTION

The optimization problems in daily life usually have non-linear features and discrete variables, which can be solved efficiently by intelligent algorithms [1], [2]. Among them, the optimal power flow (OPF) problem has great significance to the optimization and planning of power system [3]–[5]. The safe and economical operation status without any violation of system constraints can be achieved based on the power flow calculation results [6], [7]. At present, the OPF problems are mainly to minimize the power loss, fuel cost or emission separately [8]–[10]. In order to evaluate the operating status of electric system more comprehensively, the multi-objective optimal power flow (MOOPF) problems have received widespread attention.

The MOOPF problem has strict constraints and takes multiple incompatible objectives into consideration at the same time [11]–[14]. There are two key points of studying the multi-objective optimizations, one is to seek an available Pareto optimal set (POS), and the other is to determine a best compromise (BC) solution from the obtained POS. Due to the non-convex and high-dimensional features of MOOPF problems, traditional approaches may not be applicable to find a high-quality solution set. Consequently, it is imperative to utilize some appropriate intelligent algorithms to handle the MOOPF problems.

The associate editor coordinating the review of this manuscript and approving it for publication was Luca Chiaraviglio.

Recently, some evolutionary algorithms have been employed to solve the MOOPF problems successfully such as the non-dominated sorting genetic algorithm III (NSGA-III) [15], multi-objective harmony search algorithm (MOHS) [16], non-dominated sorting multi-objective opposition based gravitational search algorithm (NSMOOGSA) [17], multi-objective evolutionary algorithm based decomposition (MOEA/D) [18], hybrid DA-PSO optimization algorithm (DA-PSO) [9] and multi-objective dimension-based firefly algorithm (MODFA) [19].

The standard bat algorithm (SBA) is an innovative global optimization algorithm inspired by biological echolocation mechanism [20], [21]. Due to the simple structure and fast convergence, the standard and improved bat algorithms have been applied to various fields such as the goods distribution and job shop scheduling problems [22], [23].

The optimal solution guiding mechanism of bat algorithm enables it to deal with global optimizations such as MOOPF problems more accurately and effectively. However, the SBA algorithm is easy to fall into local optimum. In order to solve the MOOPF problems successfully, a novel hybrid bat algorithm (NHBA), which is improved by the mutation and crossover mechanisms of DE algorithm, is proposed in this paper. Meanwhile, a monotone random filling model based on extreme (MRFME) is put forward to optimize the local search manner of SBA algorithm, which is helpful to explore a better solution near the current optimal solution.

To evaluate the practicability of NHBA algorithm, some typical MOOPF simulation cases, such as the simultaneous optimization of fuel cost (with value-point loadings) and emission, the simultaneous optimization of fuel cost (with value-point loadings) and active power loss, the simultaneous optimization of fuel cost, emission and active power loss, are carried out on the IEEE 30-node, IEEE 57-node and IEEE 118-node systems. The results clearly show that the NHBA algorithm has better exploration ability than the common MOPSO and NSGA-III algorithms in finding more competitive BC solutions when utilizing the same Constrain-prior Pareto-dominance method (CPM). The detailed description of CPM can be found in literatures [24], [25].

Regrettably, the CPM method may not be very effective in solving such MOOPF problems of IEEE 57-node and IEEE 118-node systems with higher dimension. On this basis, a non-dominated sorting method with constrained Pareto fuzzy dominant (CPFD) strategy is put forward in this paper. The presented CPFD strategy gives priority to the constraints-violation value (*viol*) and then considers the fuzzy eigenvalue (Ψ), which is quite different from the typical penalty function method and CPM method. The results clearly state that the proposed sorting rule is valuable to obtain a fine-quality POS without any constraints violation in the large-scale systems.

The presented NHBA-CPFD algorithm, which combines the advantages of the NHBA algorithm and the CPFD strategy, can improve the performance of determining satisfactory POS in different scale electric systems. Moreover, the generational distance (GD) and hyper-volume (HV) metrics are employed to measure the distribution of obtained POS and the convergence to the real Pareto fronts (PF). Based on the evaluation results, the competitive superiority of NHBA-CPFD algorithm in seeking the uniformly-distributed POS can be verified.

The rest of this article is organized as follows. The mathematical model of MOOPF problem is shown in Section 2. The detailed description of NHBA algorithm is presented in Section 3. Section 4 proposes the novel CPFD strategy and a non-dominated sorting rule to seek satisfactory POS. Section 4 also generalizes the application of NHBA-CPFD algorithm on the MOOPF problems. Section 5 shows the results of ten MOOPF trials on different scale systems. The GD and HV metrics are adopted to measure the performance of obtained POS in Section 6. Section 6 also discusses the computational complexity represented by the CPU time and the dominant relationship of obtained BC solutions. Eventually, the conclusions are made in Section 7.

II. MATHEMATICAL MODEL OF MOOPF PROBLEMS

The objective functions and system constraints of MOOPF mathematical model are summarized as follows [9], [25].

$$\text{minimize} F_{obj} = (f_1(x,u), \cdots, f_i(x,u), \cdots, f_M(x,u)) \quad (1)$$

$$H_k(x,u) = 0, k = 1, 2, \cdots, h \quad (2)$$

$$G_j(x,u) \leq 0, j = 1, 2, \cdots, g \quad (3)$$

where f_i (x,u) represents the ith objective function and $M(M \geq 2)$ is the amount of objects which are optimized at the same time. H_k is the kth equality constraint (EC) and h is the amount of ECs. G_j is the jth inequality constraint (IC) and g is the total number of ICs.

The state variables x includes generator active power at slack node P_{G1}, load node voltage V_L, generator reactive power Q_G and apparent power of transmission line S. Generator active power output at PV nodeP_G, generator node voltage V_G, tap ratios of transformer T and reactive power injection Q_C are integrated into the control variables u. The vectors of x and u are described as (4) and (5).

$$x^T = \left[P_{G1}, V_{L1}, \cdots, V_{LN_{PQ}}, Q_{G1}, \cdots, Q_{GN_G}, S_1, \cdots, S_{N_L}\right] \quad (4)$$

$$u^T = \left[P_{G2}, \cdots, P_{GN_G}, V_{G1}, \cdots, V_{GN_G}, T_1, \cdots, T_{N_T}, Q_{C1}, \cdots, Q_{CN_C}\right] \quad (5)$$

where N_{PQ}, N_G, N_L, N_T and N_C indicate the amount of PQ nodes, generators, transmission lines, transformers and shunt compensators.

A. OBJECTIVE FUNCTIONS

Four objectives including the total emission, the active power loss, the basic fuel cost and the fuel cost with value-point loadings, are studied in this paper [9], [19].

1) EMISSION

$$Obj1 : F_e = \sum_{i=1}^{N_G} [\alpha_i P_{Gi}^2 + \beta_i P_{Gi} + \gamma_i + \eta_i \exp(\lambda_i P_{Gi})]\text{ton/h} \tag{6}$$

where F_e depicts the sum of emission in the unit of ton/h while α_i, β_i, γ_i, η_i and λ_i represent the emission coefficients of the ith generator.

2) ACTIVE POWER LOSS

$$Obj2 : F_P = \sum_{k=1}^{N_L} c_k[V_i^2 + V_j^2 - 2V_iV_j\cos(\delta_i - \delta_j)]\text{MW} \tag{7}$$

where F_P indicates the power loss in the unit of MW. V_i, V_j and δ_i, δ_j are, respectively, the voltage magnitude and angle at node i and node j. c_k is the conductance of the kth branch that links node i to node j.

3) BASIC FUEL COST

$$Obj3 : F_c = \sum_{i=1}^{N_G} (a_i + b_iP_{Gi} + c_iP_{Gi}^2)\$/h \tag{8}$$

where F_c is the basic fuel cost in the unit of \$/h. And a_i, b_i and c_i represent the cost coefficients of the ith generator.

4) FUEL COST WITH VALUE-POINT LOADINGS

$$Obj4 : F_{\text{c\_vp}} = \sum_{i=1}^{N_G} (a_i + b_iP_{Gi} + c_iP_{Gi}^2 + \left|d_i \times \sin(e_i \times (P_{Gi}^{\min} - P_{Gi}))\right|)\$/h \tag{9}$$

where F_{c_vp} indicates the fuel cost considering value-point loadings in the unit of \$/h. And d_i, e_i and $P_{Gi}^{\min}$ are the cost coefficients and the lower active power at the ith generator node.

B. SYSTEM CONSTRAINTS

The system constraints include equality constraints and inequality ones [26]–[28]. The optimization schemes adopted by decision-makers should not violate any *EC* and *IC*.

1) EC

The *EC*s, which can be described as (10) and (11), are essentially the power balance equations.

$$P_{Gi} - P_{Di} - V_i \sum_{j\in N_i} V_j(G_{ij}\cos\delta_{ij} + B_{ij}\sin\delta_{ij}) = 0,\ i \in N \tag{10}$$

$$Q_{Gi} - Q_{Di} - V_i \sum_{j\in N_i} V_j(G_{ij}\sin\delta_{ij} - B_{ij}\cos\delta_{ij}) = 0,\ i \in N_{PQ}$$
$$\delta_{ij} = \delta_i - \delta_j \tag{11}$$

where P_{Gi} and Q_{Gi} are the injected active and reactive power at node i. P_{Di} and Q_{Di} denote the active and reactive load demand at load node i. G_{ij} and B_{ij} denote the conductance and susceptance between the ith and jth node. N_i is the amount of nodes linked to node i and N is the number of nodes except the slack one.

2) IC

Used to define the effective operating range of electric equipment, the *IC*s include state variables and control ones.

(1) *IC*s of control variables

- active power at generator node

$$P_{Gi}^{\max} \geq P_{Gi} \geq P_{Gi}^{\min}, i \in N_G (i \neq 1) \tag{12}$$

- voltage at generator node

$$V_{Gi}^{\max} \geq V_{Gi} \geq V_{Gi}^{\min}, i \in N_G \tag{13}$$

- transformer tap-settings

$$T_i^{\max} \geq T_i \geq T_i^{\min}, i \in N_T \tag{14}$$

- reactive power injection

$$Q_{Ci}^{\max} \geq Q_{Ci} \geq Q_{Ci}^{\min}, i \in N_C \tag{15}$$

(2) *IC*s of state variables

- active power at slack node

$$P_{G1}^{\max} \geq P_{G1} \geq P_{G1}^{\min} \tag{16}$$

- voltage at load node

$$V_{Li}^{\max} \geq V_{Li} \geq V_{Li}^{\min}, i \in N_{PQ} \tag{17}$$

- reactive power at generator node

$$Q_{Gi}^{\max} \geq Q_{Gi} \geq Q_{Gi}^{\min}, i \in N_G \tag{18}$$

- apparent power

$$S_l^{\max} - S_l \geq 0, l \in N_L \tag{19}$$

III. STANDARD AND MODIFIED BAT ALGORITHMS

To overcome the premature-convergence and unsatisfactory-diversity of SBA algorithm in dealing with the MOOPF problems, the NHBA algorithm is proposed.

A. STANDARD BAT ALGORITHM

The SBA algorithm is derived based on the echolocation mechanism, and it makes bats keep close to the global optimal individual continuously by adjusting the searching frequency [20]. The frequency$fr(i)$, speed v_i and position p_i of the ith individual are defined as (20), (21) and (22), respectively [20], [29], [30].

$$fr(i) = fr_{\min} + \mu * (fr_{\max} - fr_{\min}) \tag{20}$$
$$v_i(t) = v_i(t-1) + fr(i) * (p_i(t-1) - p_{best}) \tag{21}$$
$$p_i(t) = p_i(t-1) + v_i(t) \tag{22}$$

where fr_{min} and fr_{max} limit the range of frequency. p_{best} is the current optimum individual while $\mu(\mu \in (0, 1))$ is a random number.

After the location of bat population is updated, p_{best} will be determined according to the established dominance strategy. Local search, which relies on the pulse rate R and the loudness L, aims to find a better scheme p_{per} near the p_{best} one. The update manners of L and R are shown as (23) and (24).

$$L_i(t+1) = \tau L_i(t) \tag{23}$$

$$R_i(t+1) = R_0(1 - \exp(-lt)) \tag{24}$$

where R_0 is the initial pulse rate. Two constants, $l(l > 0)$ and $\tau(\tau \in (0, 1))$, represent the increase coefficient of R and the attenuation coefficient of L. To improve the searching efficiency, L will decrease and R will increase when the p_{per} individual is found during the local search.

B. NHBA ALGORITHM

Like most global algorithms, the SBA algorithm is difficult to jump out of the local optimum. The proposed NHBA algorithm improves the performance of SBA method in the following three aspects.

1) IMPROVEMENT OF SPEED UPDATING MANNER

The non-linear weight coefficient ωc, which can enhance the population diversity, is introduced to improve the speed model of SBA algorithm. The novel updated formulas of v and ωc are defined as (25) and (26).

$$v_i(t) = \omega c(t) v_i(t-1) + r_1 fr(i)(p_{best} - p_i(t-1)) \tag{25}$$

$$\begin{aligned} \omega c(t) = {} & \omega c_{\max} - r_2(\omega c_{\max} - \omega c_{\min}) \\ & + r_3(\omega c(t-1) - (\omega c_{\max} + \omega c_{\min})/2) \end{aligned} \tag{26}$$

where $r_1 \sim r_3$ are random constants between 0 and 1. ωc_{min} and ωc_{max} set the valid range of weight coefficient.

2) INTEGRATION OF MUTATION AND CROSSOVER MECHANISMS

To search for better optimization schemes, the mutation and crossover mechanisms of DE algorithm are integrated into the NHBA algorithm. The detailed description and application of DE algorithm can be referred to literatures [31]–[33]. A new population is generated by mutation operation. The ith mutant-individual $pm(i)$ can be defined as (27).

$$pm(i) = p_{n1} + F_m(p_{n3} - p_{n2}), i = 1, 2, \cdots N_a \tag{27}$$

where p_{n1},p_{n2} and p_{n3} are three different individuals. F_m is the mutant weighting factor.

Subsequently, the bat population is cross-operated to generate the pcpopulation. The crossover mechanism can be described as (28).

$$pc(i) = \begin{cases} pm(i), & if\ ra \le F_c or j = q \\ p_i, & otherwise \end{cases} \quad j = 1, 2, \cdots, D \tag{28}$$

where $ra(ra \in (0, 1))$ is a random number and F_c is the crossover coefficient. D is the dimension of each individual and q is a random D-dimensional vector.

3) IMPROVEMENT OF LOCAL PARAMETER UPDATING MANNER

The MRFME model is put forward to improve the updated manners of two local searching parameters, which can be expressed as (29) and (30).

$$R_i = (R_{\min} - R_{\max}) * (ite - ite_{\max})/(1 - ite_{\max}) + R_{\max} \tag{29}$$

$$L_i = (L_{\max} - L_{\min}) * (ite - ite_{\max})/(1 - ite_{\max}) + L_{\min} \tag{30}$$

where ite and ite_{max} respectively indicate the current and maximum iteration. R_{min} and R_{max} limit the range of pulse rate while L_{min} and L_{max} specify the range of loudness. Undoubtedly, the proposed MRFME strategy can meet the basic requirement of bat algorithm, which requires the increasing pulse and decreasing loudness when the p_{per} individual is accepted as the new optimal solution.

The pseudo codes of the innovative NHBA algorithm for the minimization problems are summarized in Table 1.

IV. MULTI-OBJECTIVE OPTIMIZATION STRATEGIES

The penalty function method is commonly used to select feasible POS when dealing with the MOOPF problems. However, it is difficult to determine the appropriate penalty coefficients and ensure every solution meet all system constraints. Then, the CPM method which measures the solution-performance by objective and constraints-violation values is proposed [24], [25]. The striking advantage of CPM method is that it achieves zero-violation of obtained POS. Compared with CPM method, the proposed CPFD strategy, which takes both the fuzzy eigenvalue and the constraints-violation into consideration, can seek more favorable Pareto non-inferior solutions in IEEE 57-node and IEEE 118-node systems.

A. CONSTRAINED PARETO FUZZY DOMINANT RULE

The high-quality POS should realize none-violation of *EC*s and *IC*s. The *EC*s can be satisfied when calculating the Newton-Raphson power flow. The control variables of the ith individual which violates the *IC*s can be adjusted as (31).

$$u_i = \begin{cases} u_i^{\max} & if\ u_i > u_i^{\max} \\ u_i^{\min} & if\ u_i < u_i^{\min} \end{cases} \tag{31}$$

The CPFD strategy is proposed to handle the unqualified state variables. Generally speaking, the smaller constraints-violation value means the higher adoption-priority of corresponding individual. The key steps to judge the dominant relationship of two different solutions are arranged as follows.

(i) Clarify the violation of the ith solution based on (32).

$$viol(u_i) = \sum_{j \in c} \max(G_j(x, u_i), 0) c \in g \tag{32}$$

where c is the amount of *IC*s on state variables.

TABLE 1. Pseudo codes of NHBA algorithm.

input: objective function: $f(x)$,x=$[x_1,x_2,\ldots,x_D]^T$
the initial parameters of NHBA algorithm: the size of bat population N_a, the maximum iteration ite_{max}, the mutant factor F_m, the crossover coefficient F_c, the range of frequency $[fr_{min}, fr_{max}]$, the ranges of loudness $[L_{min}, L_{max}]$ and pulse rate $[R_{min}, R_{max}]$
Begin
ite=1
while $ite < ite_{max}$
Update the speed and position of bat population based on (25) and (22) to generate the *Xpopulation* population;
Calculate the fitness $f_x(p_i)$ (i=1,2,…,N_a) of each individual in the *Xpopulation* population;
Complete the mutation and crossover operations in the *Xpopulation* population to generate the *Ypopulation* population;
Calculate the fitness $f_y(p_i)$ (i=1,2,…,N_a) of each individual in the *Ypopulation* population;
for i=1,2,…,N_a
if $f_x(p_i) \leqslant f_y(p_i)$
Fpopulation(i)= *Xpopulation*(i);
else
Fpopulation(i)= *Ypopulation*(i);
end
Calculate the fitness $f(p_i)$ *of* ith individual in the the *Fpopulation* population;
end
Determine the current optimal individual p_{best} in *Fpopulation population*;
for ith (i=1,2,…,N_a) individual in *Fpopulation* population
Generate a random number between 0 and 1 named *rand1*.
if *rand1*>R_i
Generate the p_{per} individual which is around the p_{best} individual by a random perturbation;
Generate other random number between 0 and 1 named *rand2* and evaluate $f(p_{per})$;
if (*rand2*<L_i) && ($f(p_{per}) < f(p_{best})$)
The new individual p_{per} will be accepted as the new current optimal solution;
Update R_i and L_i based on (29) and (30);
end if
end if
end for
Renovate the information of the p_{best} solution;
ite=ite+1;
end while
End
output: p_{best} and $f(p_{best})$

(ii) Compare the values of $viol\,(u_1)$ and $viol\,(u_2)$, where $u_1(u_1 = (U_1,U_2,\ldots,U_D))$ and $u_2(u_2 = (V_1,V_2,\ldots,V_D))$ are two different sets of control variables.

(iii) When the condition (33) or (34) can be satisfied, the judgment can be made that u_1 will dominate u_2.

$$viol(u_1) < viol(u_2) \tag{33}$$

$$(viol(u_1) = viol(u_2)) \cap (\psi(u_1) > \psi(u_2)) \tag{34}$$

where $\psi\,(u_i)$ is the fuzzy eigenvalue of u_i which can be calculated as follows.

$$P(u_1) = u_1 - u_2 = (U_1 - V_1, \cdots, U_D - V_D) \tag{35}$$

$$\varphi(u_1) = F_M(P(u_1)) = (\varphi_1^{u_1}, \cdots, \varphi_D^{u_1}) \tag{36}$$

$$\psi(u_1) = \varphi_1^{u_1} \times \varphi_2^{u_1} \times \cdots \varphi_D^{u_1} \tag{37}$$

$$F_M = \begin{cases} 1, & x \leq -1 \\ \vartheta_1 x^3 + \vartheta_2, & -1 < x < 1\ \vartheta_1 = -1/2, \vartheta_2 = -\vartheta_1 \\ 0, & x \geq 1 \end{cases} \tag{38}$$

where $P(u_1)$ is the performance of u_1 relative to u_2. F_M is the adopted fuzzy membership function which can be expressed as (38).$\varphi\,(u_1)$ represents the dominant degree of u_1 relative to u_2. $\psi\,(u_i)$ is actually the product of each dominance degree.

B. NON-DOMINATED SORTING RULE BASED ON THE CPFD STRATEGY

A reasonable technology of dealing with the multi-objective optimization such as aero-assisted vehicle trajectory planning is to assign priority factors to different objectives according to the mission scenarios or the requirements of decision-makers [32], [34]. Specifically, the priority factor of primary task should be higher than the others.

The sorting rule proposed to handle the MOOPF problem does not assign objective-priority factors in advance, but determines the adoption-priority according to the *rank* index and the Pareto fuzzy dominant fitness *(cpfdf)* value of each control variable set.

In detail, the *rank* index which is essential to the presented sorting rule can be determined based on mentioned CPFD strategy.

1) RANK INDEX

In order to select high-performance Pareto solutions in multi-objective optimization problems, it is necessary to set a pre-specified priority requirement to rank candidate solutions. In this paper, the CPFD strategy which clarifies the *viol* and Ψ values is used to determine the *rank* index.

Learning from the non-dominated sorting method proposed by Kalyanmoy Deb [35], [36], the *rank* of each individual can be clarified as follows.

(i) Firstly, a hybrid population (*HP)* is composed of the parent bat population (*PBP)* with size of N_a and the external archive population (*EAP)* with size of N_a.
(ii) According to the CPFD strategy, these solutions which are not dominated by other solutions in *HP* are determined and marked as *rank*=1.
(iii) Eliminate the individuals with *rank*=1. Based on the same CPFD dominant relationship, another set of non-inferior solutions which will be marked as *rank*=2 is found.
(IV) Repeat the above operation till each individual in *HP* has its own *rank* index.

2) CPFDF INDEX

To gain an evenly-distributed PF, the *cpfdf* index is taken into account as well. The core steps to determine the *cpfdf* index of each solution can be arranged as follows.

In the *HP* population with $2N_a$ individuals, the ith ($i = 1, 2, \ldots, 2N_a$) individual can be combined with the other ($2N_a-1$) individuals. For two different individuals i and j ($j = (1, 2, \ldots, 2N_a) \cap j \neq i$), the fuzzy eigenvalue of i relative to j (Ψ_{ij}) and the fuzzy eigenvalue of j relative to i (Ψ_{ji}) can be obtained based on (37). Then, the standard performance of i relative to j named as H_{ij} can be calculated according to formula (39). On this basis, the *cpfdf*index can be determined

based on (40).

$$H_{ij} = {\Psi_{ij}}/{(\Psi_{ij} + \Psi_{ji})} \tag{39}$$

$$cpfdf(i) = \sum^{j} {Hij}/{2N_a - 1}, j = 1, 2, \cdots 2N_a \cap j \neq i \tag{40}$$

where *cpfdf(i)* represents the Pareto fuzzy dominant fitness of the *i*th individual relative to the other ($2N_a$-1) individuals. It is actually the mean value of standard performance.

The priority of each individual can be determined based on the suggested non-dominated sorting strategy. In detail, the *i*th individual has higher adoption-priority than the *j*th one when condition (41) or (42) can be met.

$$rank(i) < rank(j) \tag{41}$$

$$rank(i) = rank(j) \cap cpfdf(i) > cpfdf(j) \tag{42}$$

The individuals which ranked in the former N_a are the obtained POS based on the CPFD strategy and they will form the new *EAP*population.

The obvious difference from the sorting method of NSGA-II algorithm [35] is that, the suggested sorting rule based on CPFD strategy considers the *cpfdf* value instead of the common-used crowding distance. This novel sorting rule is very advantageous to select a satisfactory POS set in large-scale systems such as the IEEE 57-node and IEEE 118-node systems.

3) FAA APPROACH

Taking advantage of the proposed sorting strategy, a set of Pareto non-inferior solutions can be achieved. The FAA approach employed in this paper is to pick out a feasible BC solution from the obtained POS [19].

The satisfaction of the *i*th objective function for the *z*th individual ($sat_i(z)$) and the total satisfaction value of the *z*th Pareto solution ($tots(z)$) are defined as (43) and (44), respectively.

$$sat_i(z) = \begin{cases} 1 & f_i \leq f_i^{\min} \\ \dfrac{f_i^{\max} - f_i}{f_i^{\max} - f_i^{\min}} & f_i^{\min} < f_i < f_i^{\max} \\ 0 & f_i \geq f_i^{\max} \end{cases}$$
$$z = 1, 2, \ldots N_a i = 1, 2, \ldots, M \tag{43}$$

$$tots(z) = \frac{\sum_{i=1}^{M} sat_i(z)}{\sum_{z=1}^{N_a} \sum_{i=1}^{M} sat_i(z)} \tag{44}$$

where $f_i^{\max}$ and $f_i^{\max}$ are the maximum and minimum of the *i*th objective.

Calculate the *tots* index of each Pareto solution to determine the special solution which has the highest satisfaction, as known as the BC solution achieved by the FAA method.

C. APPLICATION OF NHBA-CPFD ALGORITHM ON MOOPF PROBLEMS

The NHBA-CPFD algorithm combines the great strengths of both the NHBA algorithm and the novel non-dominated sorting rule, which is the integration of two multi-objective strategies proposed in this paper.

To evaluate the powerful competitiveness of NHBA-CPFD algorithm, in contrast to MOPSO and NSGA-III methods, both bi-objective and tri-objective optimization trials are studied. Details of all cases involved in this paper are shown in Table 2. The mathematical model of objective functions is described in Section 2.

The application of NHBA-CPFD algorithm on MOOPF problems can be summarized in Figure 1.

The initial *PBP* population is randomly generated according to (45). Each bat individual is essentially a set of *D*-dimensional control variables in the power system. Designate the initial global optimal individual p_{best}randomly.

$$u_i = u_i^{\min} + rand\left(u_i^{\max} - u_i^{\min}\right)$$
$$i \in [1, N_a], u_i = [u_i^1, u_i^2, \cdots, u_i^D] \tag{45}$$

where $u_i^{\min}$ and $u_i^{\min}$ limit the range of control variables.

By adjusting the corresponding electrical equipment according to the control variables of obtained BC solutions, the system can achieve the predetermined operation state. And it is the practical significance of devoting great effort in studying the MOOPF problems.

V. SIMULATION AND RESULTS

The MATLAB 2014a software is employed and all testing cases in this paper are run on a PC with Intel(R) Core(TM) i5–7500 CPU @ 3.40 GHz with 8GB RAM.

A. SYSTEMS

For a comprehensive evaluation of the presented NHBA-CPFD algorithm, ten simulation trials are carried out on three different scale systems.

The structure of IEEE 30-node system is shown in Figure 2 and the details are shown in Table 3. More information can be found in [19], [37] and Table 4 gives the coefficients of fuel cost and emission.

The structure of IEEE 57-node is shown in Figure 3 and the details are obtained from [19]. The transformer taps and voltage magnitude for the PQ and PV nodes are bound in 0.9-1.1p.u. . The shunt capacitor is restricted in 0-0.3p.u.. Table 5 shows the coefficients of fuel cost and emission in IEEE 57-node system.

The single line diagram of IEEE 118-node system with 128-dimensional control variables is shown in Figure 4. The bound of voltage magnitude for PV node is set as 0.9-1.1 p.u. and the shunt capacitor is restricted in 0-0.3 p.u.. The other details of IEEE 118-node system can be found in [19].

B. ALGORITHM PARAMETERS

In order to figure out the influence of main algorithm parameters on optimization performance and determine a set of relatively optimal combination, a bi-objective case which aims to optimize the basic fuel cost and emission at the same time is taken as an example.

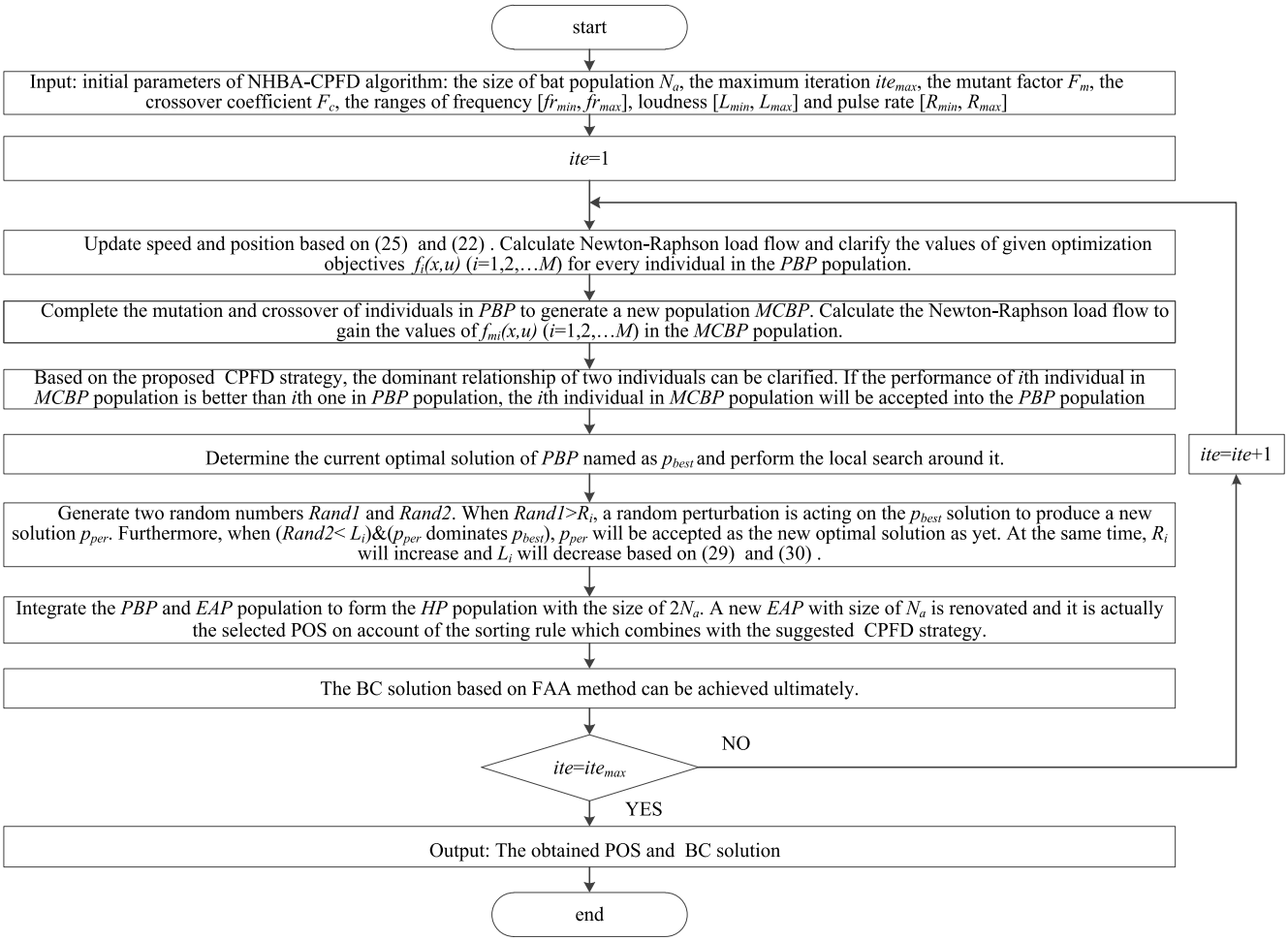

FIGURE 1. The flow chart of NHBA-CPFD algorithm on MOOPF problems.

TABLE 2. Objective combination.

	Obj1	*Obj2*	*Obj3*	*Obj4*	Test system
CASE1	✔		✔		IEEE 30
CASE2		✔	✔		IEEE 30
CASE3	✔			✔	IEEE 30
CASE4		✔		✔	IEEE 30
CASE5	✔	✔	✔		IEEE 30
CASE6	✔	✔		✔	IEEE 30
CASE7	✔		✔		IEEE 57
CASE8		✔	✔		IEEE 57
CASE9	✔		✔		IEEE 118
CASE10		✔	✔		IEEE 118

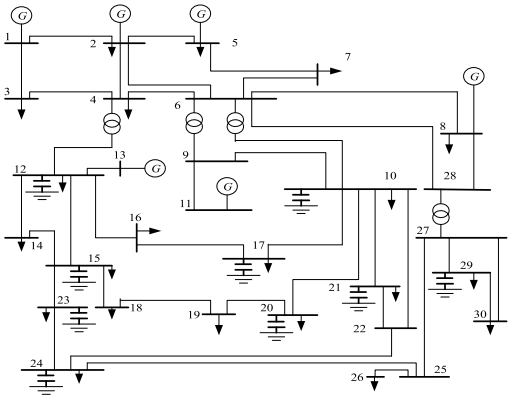

FIGURE 2. Structure of the IEEE 30-node system.

In detail, the influences of the maximum iteration and the valid range of ωc are studied in this paper. The results are achieved by NHBA-CPFD algorithm with a population size of 100.

Figure 5 shows the PFs with different maximum iterations. It clearly indicates that the iteration of 100 obtains the worst PF while the iteration of 200,300 and 400 can achieve better PFs. Figure 5 also validates that the iterations of 500 and 600 are capable to achieve well-distributed PFs with similar efficiency. To reduce the computational time, the maximum iteration in this paper is set as 500.

Then, the influence of ωc is discussed. Figure 6 shows the PFs based on the different minimum value of ωc when the top-limit is set as $\omega c_{max} = 0.95$. It states that the ωc_{min} of 0.1 gets the worse distribution and the ωc_{min} of 0.4 achieves the best one. Figure 7 shows the PFs based on

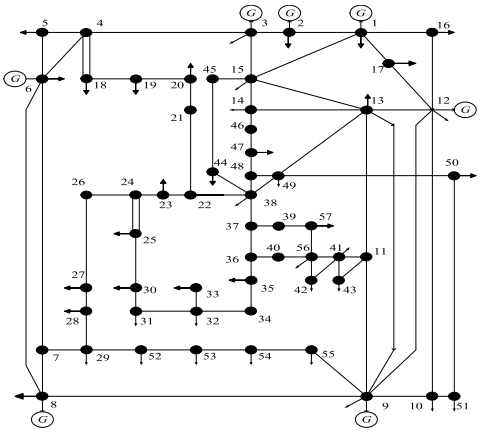

FIGURE 3. Structure of the IEEE 57-node system.

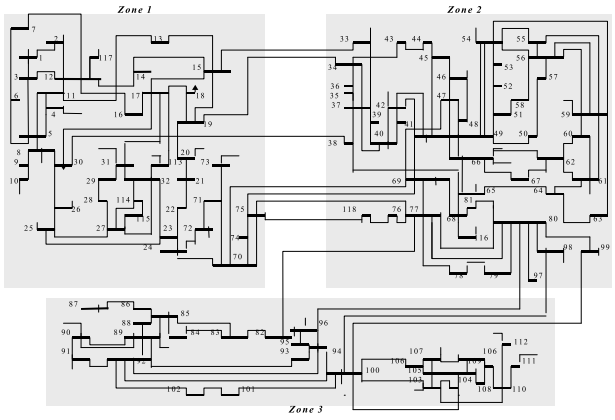

FIGURE 4. Structure of the IEEE 118-node system.

different maximum value of ωc when the lower-limit is set as $\omega c_{min} = 0.4$. It indicates that the ωc_{max} of 0.92 gets the worse distribution while the ωc_{max} of 0.9 achieves a better PF. Therefore, it is reasonable to infer that the appropriate range of the non-linear weight coefficient is [0.4, 0.9].

Additionally, the other parameters of four involved algorithms are shown in Table 6.

C. TRIALS ON IEEE 30-NODE SYSTEM

Four bi-objective and two tri-objective testing trials are performed on the IEEE 30-node system.

1) CASE1 CONSIDERING BASIC FUEL COST AND EMISSION SIMULTANEOUSLY

In *CASE1*, two objectives of F_c and F_e are optimized concurrently by the presented NHBA, NHBA-CPFD, MOPSO and NSGA-III approaches. The obtained PFs are shown in Figure 8 and it indicates that the NHBA and NHBA-CPFD algorithms can obtain preferable POS than MOPSO and NSGA-III methods. Even further, the NHBA-CPFD algorithm has great potential to find more favorable PF than NHBA algorithm.

The 24-dimensional control variables of BC solution obtained by four algorithms are given in Table 7. Table 7 also lists two boundary solutions found by NHBA-CPFD algorithm including *C1.E* (the solution with minimum emission) and *C1.F* (the solution with minimum fuel cost). More specifically, the BC solution obtained by NHBA algorithm includes 0.2375 ton/h of F_e and 832.6471 \$/h of F_c and the BC solution obtained by NHBA-CPFD algorithm includes 0.2350 ton/h of F_e and 830.9592 \$/h of F_c. In addition, the *C1.E*includes 0.1943 ton/h of minimal F_e and 955.0343 \$/h of F_c. The *C1.F* includes 0.3309 ton/h of F_e and 799.7640 \$/h of minimal F_c.

In order to make the conclusion that the NHBA-CPFD algorithm can effectively handle MOOPF problems more persuasiveness, Table 8 gives the comparison results between the proposed algorithms and other methods.

2) CASE2 CONSIDERING BASIC FUEL COST AND ACTIVE POWER LOSS SIMULTANEOUSLY

In *CASE2*, two competing objectives of F_c and F_p are studied. The PFs obtained by four algorithms are shown in Figure 9.

Table 9 gives the control variables of BC solutions and the comparison results shown in other literatures. Table 9 also lists two boundary solutions found by NHBA-CPFD algorithm including *C2.F* (the solution with minimum fuel cost) and *C2.P* (the solution with minimum power loss). As can be seen from Table 9, the BC solution obtained by NHBA algorithm includes 835.1034 \$/h of F_c and 5.0658 MW of F_p. The BC solution obtained by NHBA-CPFD algorithm includes 831.8513 \$/h of F_c and 5.1096 MW of F_p. Besides, the *C2.F*includes 799.3296 \$/h of minimal F_c and 8.5486 MW of F_p. The *C2.P*includes 966.8891 \$/h of F_c and 2.9023 MW of minimalF_p.

3) CASE3 CONSIDERING FUEL COST WITH VALUE-POINT AND EMISSION SIMULTANEOUSLY

In *CASE3*, two objectives of F_{c-vp} and F_e are optimized simultaneously. The PFs respectively obtained by different algorithms are shown in Figure 10.

Table 10 shows the control variables of BC solutions achieved by four involved methods. Table 10 also lists two boundary solutions found by NHBA-CPFD algorithm including *C3.Fv* (the solution with minimum fuel cost with value-point) and *C3.E* (the solution with minimum emission).

In detail, Table 10 clearly states that the BC solution obtained by NHBA algorithm includes 854.3882 \$/h of F_{c-vp} and 0.2598 ton/h of F_e. The BC solution obtained by NHBA-CPFD algorithm includes 855.5369 \$/h of F_{c-vp} and 0.2585 ton/h of F_e. In addition, the *C3.Fv*includes 831.6332 \$/h of minimal F_{c-vp} and 0.3727 ton/h of F_e. And the *C3.E* includes 1023.2904 \$/h of F_{c-vp} and 0.1944 ton/h of minimal F_e.

4) CASE4 CONSIDERING FUEL COST WITH VALUE-POINT AND ACTIVE POWER LOSS SIMULTANEOUSLY

In *CASE4*, the F_{c-vp} and F_p are optimized concurrently and the obtained PFs are shown in Figure 11. The control variables of BC solutions are listed in Table 11. Table 11 also shows two boundary solutions found by NHBA-CPFD

TABLE 3. Details of the IEEE 30-node system.

equipment	amount	details
nodes	30	-
branches	41	-
generators	6	nodes:1,2,5,8,11,and13
transformer taps	4	branches:6-9,6-10,4-12 and 28-27 limit: 0.9p.u.-1.1p.u.
capacitors	9	nodes:10,12,15,17,20,21,23,24 and 29
control variables	24	-
voltage of generator nodes	-	limit: 0.95p.u.-1.1p.u
voltage of load nodes	-	limit: 0.95p.u.-1.1p.u

TABLE 4. Fuel and emission coefficients of the IEEE 30-node system.

coefficient	Generating unit					
	G1	G2	G5	G8	G11	G13
Fuel cost						
a	0	0	0	0	0	0
b	2	1.75	1	3.25	3	3
c	0.00375	0.0175	0.0625	0.00834	0.025	0.025
d	18	16	14	12	13	13.5
e	0.037	0.038	0.04	0.045	0.042	0.041
Emission						
α	0.06490	0.05638	0.04586	0.03380	0.04586	0.05151
β	-0.05554	-0.06047	-0.05094	-0.03550	-0.05094	-0.05555
γ	0.04091	0.02543	0.04258	0.05326	0.04258	0.06131
η	0.0002	0.0005	0.000001	0.002	0.000001	0.00001
λ	2.857	3.333	8.000	2.000	8.000	6.667

TABLE 5. Fuel and emission coefficients of the IEEE 57-node system.

coefficient	Generating unit						
	G1	G2	G3	G6	G8	G9	G12
Fuel cost							
a	0	0	0	0	0	0	0
b	20	40	20	40	20	40	20
c	0.0775795	0.01	0.25	0.01	0.0222222	0.01	0.0322581
Emission							
α	0.06	0.05	0.04	0.035	0.045	0.05	0.05
β	-0.05	-0.06	-0.05	-0.03	-0.05	-0.04	-0.05
γ	0.04	0.03	0.04	0.035	0.05	0.045	0.06
η	0.00002	0.00005	0.00001	0.00002	0.00004	0.00001	0.00001
λ	0.5	1.5	1	0.5	2	2	1.5

algorithm including *C4.Fv* (the solution with minimum fuel cost with value-point) and *C4.P* (the solution with minimum power loss). As can be seen from Table 11, the BC solution achieved by NHBA algorithm includes 868.9526 $/h of F_{c-vp} and 5.6761 MW of F_p. The BC solution obtained by NHBA-CPFD algorithm includes 865.9106 $/h of F_{c-vp} and 5.6726 MW of F_p. Besides, the *C4.Fv* includes 833.3204 $/h of minimal F_{c-vp} and 10.4024 MW of F_p. The *C4.P* includes 1022.0654 $/h of F_{c-vp} and 2.9227 MW of minimal F_p.

5) CASE5 CONSIDERING FUEL COST, ACTIVE POWER LOSS AND EMISSION SIMULTANEOUSLY

To certify the superiority of proposed NHBA-CPFD algorithm comprehensively, the more difficult optimization trials with three objectives are studied in this paper.

In *CASE5*, three competing objectives of F_c, F_p and F_e are optimized concurrently. The PFs respectively obtained by MOPSO, NSGA-III, NHBA and NHBA-CPFD algorithms are shown in Figure 12. Table 12 shows the control variables of achieved BC solutions and three boundary solutions found by NHBA-CPFD algorithm including *C5.F* (the solution with minimum fuel cost), *C5.P* (the solution with minimum power loss) and *C5.E* (the solution with minimum emission). It intuitively states that the BC solution obtained by NHBA algorithm includes 868.7380 $/h of F_c, 4.1744 MW of F_p and 0.2111 ton/h of F_e. The BC solution obtained

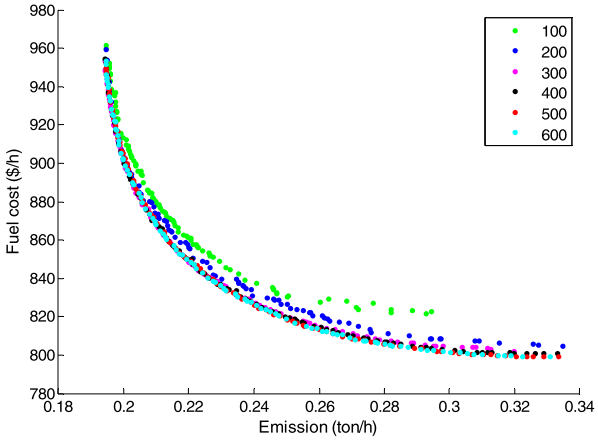

FIGURE 5. PFs based on different maximum iterations.

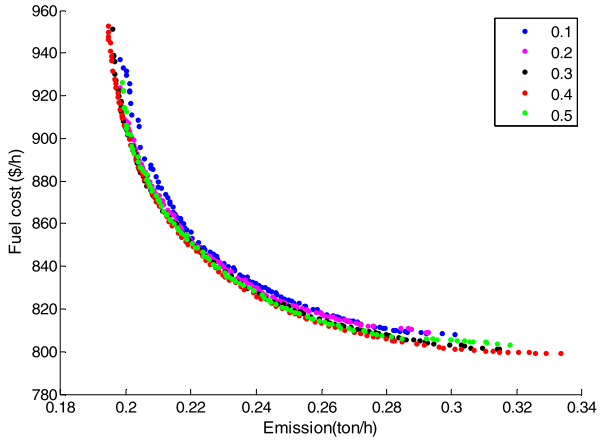

FIGURE 6. PFs based on different minimum value of ωc.

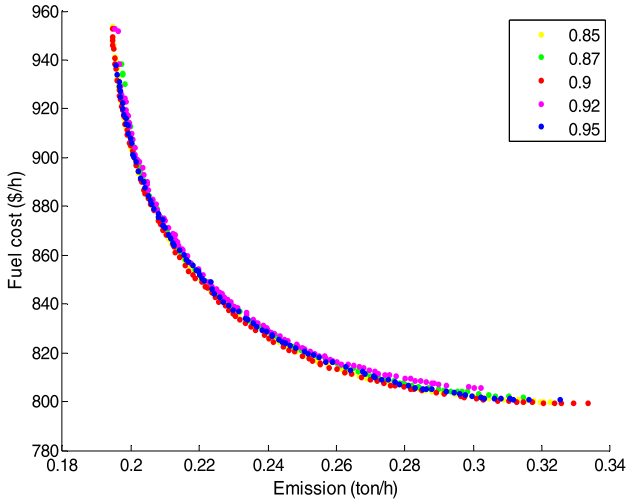

FIGURE 7. PFs based on different maximum value of ωc.

by NHBA-CPFD algorithm includes 865.4229 \$/h of F_c, 4.3535 MW of F_p and 0.2116 ton/h of F_e.

In addition, the *C5.F* includes 799.3578 \$/h of minimal F_c. The *C5.E* includes 0.1943 ton/h of minimal F_e and the *C5.P* includes 3.0176 MW of minimal F_p.

6) CASE6 CONSIDERING FUEL COST WITH VALUE-POINT, ACTIVE POWER LOSS AND EMISSION SIMULTANEOUSLY

In *CASE6*, three objectives of F_{c-vp}, F_p and F_e are optimized concurrently and the obtained PFs are shown in Figure 13. The control variables of BC solutions obtained by NHBA and NHBA-CPFD algorithms, compared with the results obtained by MOPSO and NSGA-III methods, are shown in Table 13.

For *CASE6*, three boundary solutions found by NHBA-CPFD algorithm including *C6.Fv* (the solution with minimum fuel cost with value-point), *C6.P* (the solution with minimum power loss) and *C6.E* (the solution with minimum emission) are listed on Table 13 as well.

More specifically, the BC solution achieved by NHBA algorithm includes 964.8493 \$/h of F_{c-vp}, 3.9018 MW of F_p and 0.2047 ton/h of F_e. The BC solution achieved by

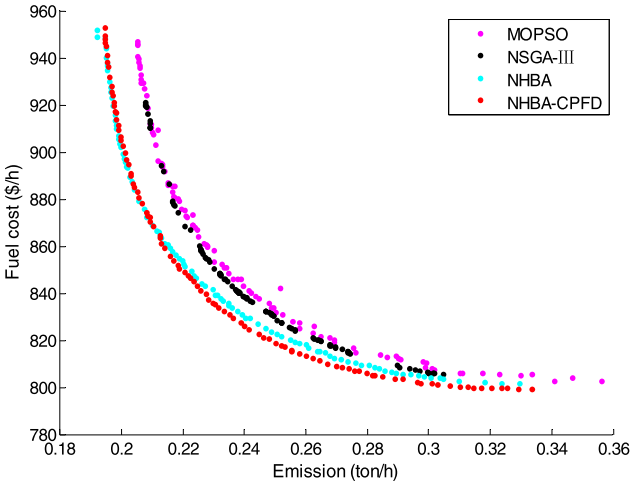

FIGURE 8. PFs obtained by different algorithms for *CASE1*.

NHBA-CPFD algorithm includes 962.8123 \$/h of F_{c-vp}, 3.9637 MW of F_p and 0.2041 ton/h of F_e. Besides, the *C6.Fv* includes 904.6377 \$/h of minimal F_{c-vp}. The *C6.E* includes 0.1943 ton/h of minimal F_e and the *C6.P*includes 2.9541 MW of minimal F_p.

D. TRIALS ON IEEE 57-NODE SYSTEM

To explore the universal applicability of proposed NHBA-CPFD algorithm, simulation cases of MOOPF problems on the IEEE 57-node system are discussed.

1) CASE7 CONSIDERING BASIC FUEL COST AND EMISSION SIMULTANEOUSLY

In *CASE7*, two objectives of F_c and F_e are optimized simultaneously. The obtained PFs are shown in Figure 14. In addition, the 33-dimensional control variables of BC solutions and two boundary solutions (*C7.F* and *C7.E*) found by NHBA-CPFD algorithm are shown in Table 14. In detail, the BC solution achieved by NHBA algorithm includes 43244.5741 \$/h of F_c and 1.2192 ton/h of F_e. The BC solution obtained by NHBA-CPFD algorithm includes 43221.5876 \$/h of F_c and 1.2164 ton/h of F_e. In addition, the *C7.F* includes 41678.6457 \$/h of minimal F_c and 1.6319 ton/h of F_e. The *C7.E* includes 48186.3156 \$/h of F_c and 1.0271 ton/h of minimal F_e.

2) CASE8 CONSIDERING BASIC FUEL COST AND ACTIVE POWER LOSS SIMULTANEOUSLY

In *CASE8*, two objectives of F_c and F_p are optimized simultaneously. The PFs respectively achieved by the NBHA-CPFD algorithm and the other three methods are shown in Figure 15. Table 15 gives the control variables of obtained BC solutions and two boundary solutions (*C8.F* and *C8.P*) found by NHBA-CPFD algorithm. As can be seen from Table 15, the BC solution obtained by NHBA algorithm includes 41934.2468 \$/h of F_c and 11.0174 MW of F_p. The BC solution achieved by NHBA-CPFD algorithm includes

TABLE 6. Main parameters of MOPSO, NSGA-III, NHBA and NHBA-CPFD algorithms.

parameters	MOPSO	NSGA-III	NHBA/NHBA-CPFD
size of population	100	100	100
size of *EAP*	100	100	100
maximum iterations	500	500	500
c1/*c2*	2	--	--
mutation indictor/ percentage	--	20/1	--
crossover indictor/ percentage	--	20/0.1	--
number of divisions	--	10	--
mutant weighting factor F_m	--	--	0.6
crossover coefficient F_c	--	--	0.8
ωc(min/max)	--	-	0.4/0.9
fr(min/max)	--	--	0/2
R(min/max)	--	--	0.1/0.5
L(min/max)	--	--	0.5/0.95

TABLE 7. Specific solutions and control variables of CASE1.

control variables	MOPSO	NSGA-III	NHBA	NHBA-CPFD	*C1.E*	*C1.F*	BSA [38]
P_{G2}(MW)	59.3113	56.9231	58.1990	58.3448	73.4104	47.9982	59.3719
P_{G5}(MW)	25.3313	28.6463	25.6741	26.0838	50.0000	20.9138	27.6576
P_{G8}(MW)	32.1623	34.7837	27.0218	34.3432	35.0000	20.5543	34.9989
P_{G11}(MW)	24.3430	28.6194	26.3626	26.0900	30.0000	12.6536	27.0652
P_{G13}(MW)	29.2546	26.0422	31.3704	26.3332	40.0000	12.0000	26.4502
V_{G1}(p.u.)	1.0948	1.1000	1.1000	1.1000	1.0596	1.1000	1.1000
V_{G2}(p.u.)	1.0839	1.0805	1.0890	1.0931	1.0483	1.0887	1.0855
V_{G5}(p.u.)	1.0417	1.0649	1.0537	1.0564	1.0233	1.0648	1.0606
V_{G8}(p.u.)	1.0686	1.0654	1.0639	1.0545	1.0326	1.0730	1.0757
V_{G11}(p.u.)	1.0738	1.0913	1.0880	1.0724	1.0618	1.0534	1.1000
V_{G13}(p.u.)	1.0875	1.0945	1.0517	1.0946	1.0733	1.0516	1.1000
T_{11}(p.u.)	1.1000	0.9225	1.0711	0.9900	0.9609	1.0027	1.0000
T_{12}(p.u.)	1.0848	1.0482	0.9304	0.9135	1.0032	1.0094	0.9500
T_{15}(p.u.)	0.9890	0.9844	1.1000	1.0032	0.9670	1.0280	1.0000
T_{36}(p.u.)	1.0067	1.0127	1.0097	0.9414	1.0231	1.0213	0.9625
Q_{C10}(p.u.)	0.0423	0.0103	0.0299	0.0297	0.0303	0.0232	3.4844(Mvar)
Q_{C12}(p.u.)	0.0086	0.0348	0.0473	0.0043	0.0203	0.0072	4.5129(Mvar)
Q_{C15}(p.u.)	0.0234	0.0225	0.0157	0.0202	0.0137	0.0161	4.7990(Mvar)
Q_{C17}(p.u.)	0.0229	0.0043	0.0450	0.0296	0.0149	0.0201	4.9965(Mvar)
Q_{C20}(p.u.)	0.0018	0.0493	0.0291	0.0357	0.0298	0.0103	3.9809(Mvar)
Q_{C21}(p.u.)	0.0000	0.0384	0.0333	0.0042	0.0308	0.0243	4.7684(Mvar)
Q_{C23}(p.u.)	0.0435	0.0120	0.0500	0.0236	0.0139	0.0077	3.8535(Mvar)
Q_{C24}(p.u.)	0.0500	0.0381	0.0235	0.0500	0.0401	0.0398	4.2332(Mvar)
Q_{C29}(p.u.)	0.0337	0.0380	0.0088	0.0261	0.0400	0.0474	1.6339(Mvar)
Emission(ton/h)	0.2500	0.2423	**0.2375**	**0.2350**	**0.1943**	0.3309	0.2425
Fuel cost($/h)	832.1254	836.4405	**832.6471**	**830.9592**	955.0343	**799.7640**	835.0199

TABLE 8. Comparison results of BC solutions for CASE1.

comparison	Fuel cost($/h)	Emission(ton/h)
NHBA	832.6471	0.2375
NHBA-CPFD	830.9592	0.2350
BSA [38]	835.0199	0.2425
MOEA/D [18]	833.72	0.2438
ESDE-MC [39]	830.7185	0.2483
MGBICA [40]	830.8514	0.2484
AGSO [41]	843.5473	0.2539

41925.5743 $/h of F_c and 10.9884 MW of F_p. Besides, the *C8.P* includes 43052.0891 $/h of F_c and 9.9299 MW of minimal F_p. And the *C8.F* includes 41655.1128 $/h of minimal F_c and 14.4357 MW of F_p.

E. TRIALS ON IEEE 118-NODE SYSTEM

The IEEE 118-node system is employed to evaluate the effectiveness of proposed NHBA-CPFD algorithm on larger scale systems.

TABLE 9. Specific solutions and control variables of CASE2.

control variables	MOPSO	NSGA-III	NHBA	NHBA-CPFD	*C2.F*	*C2.P*	MOEA/D [18]
P_{G2}(MW)	80.0000	51.3612	54.7737	52.6991	49.4563	80.0000	53.572
P_{G5}(MW)	25.9706	32.5928	34.1273	32.0940	21.8309	50.0000	32.890
P_{G8}(MW)	35.0000	34.1453	35.0000	34.9082	22.1551	35.0000	34.993
P_{G11}(MW)	11.1284	28.9390	26.3571	26.9260	11.4655	30.0000	28.244
P_{G13}(MW)	20.7805	20.8168	20.5383	22.2317	12.0000	39.8845	21.963
V_{G1}(p.u.)	1.1000	1.0187	1.0993	1.1000	1.1000	1.1000	1.1000
V_{G2}(p.u.)	1.0888	1.0059	1.0857	1.0912	1.0884	1.0981	1.0920
V_{G5}(p.u.)	1.0806	0.9810	1.0629	1.0683	1.0629	1.0788	1.0690
V_{G8}(p.u.)	1.0746	0.9923	1.0749	1.0762	1.0684	1.0940	1.0793
V_{G11}(p.u.)	1.1000	1.0884	1.0754	1.1000	1.1000	1.0930	1.1000
V_{G13}(p.u.)	1.1000	1.0622	1.0984	1.1000	1.0950	1.0921	1.0999
T_{11}(p.u.)	1.1000	0.9293	0.9911	0.9954	1.0580	0.9759	1.0617
T_{12}(p.u.)	0.9000	0.9645	0.9871	0.9444	0.9035	1.0230	0.9000
T_{15}(p.u.)	1.0338	0.9569	0.9802	0.9918	1.0116	1.0116	0.9953
T_{36}(p.u.)	0.9978	0.9246	0.9628	0.9852	0.9983	0.9866	0.9700
Q_{C10}(p.u.)	0.0182	0.0433	0.0169	0.0098	0.0079	0.0329	5.000(Mvar)
Q_{C12}(p.u.)	0.0182	0.0194	0.0000	0.0246	0.0491	0.0411	5.000(Mvar)
Q_{C15}(p.u.)	0.0500	0.0464	0.0297	0.0500	0.0448	0.0458	4.503(Mvar)
Q_{C17}(p.u.)	0.0299	0.0154	0.0391	0.0074	0.0000	0.0393	5.000(Mvar)
Q_{C20}(p.u.)	0.0361	0.0473	0.0108	0.0031	0.0100	0.0242	4.592(Mvar)
Q_{C21}(p.u.)	0.0495	0.0210	0.0500	0.0251	0.0184	0.0389	4.960(Mvar)
Q_{C23}(p.u.)	0.0430	0.0422	0.0264	0.0201	0.0141	0.0097	3.069(Mvar)
Q_{C24}(p.u.)	0.0003	0.0102	0.0500	0.0430	0.0396	0.0500	4.994(Mvar)
Q_{C29}(p.u.)	0.0491	0.0148	0.0500	0.0412	0.0283	0.0261	2.500(Mvar)
Fuel cost($/h)	837.6251	835.0259	**835.1034**	**831.8513**	**799.3296**	966.8891	835.36
Power loss(MW)	5.9861	5.9213	**5.0658**	**5.1096**	8.5486	**2.9023**	4.9099

TABLE 10. Specific solutions and control variables of CASE3.

control variables	MOPSO	NSGA-III	NHBA	NHBA-CPFD	*C3.Fv*	*C3.E*
P_{G2}(MW)	78.6222	59.7779	63.1732	60.6335	43.0864	73.6854
P_{G5}(MW)	17.8190	23.8525	26.6166	22.6786	19.3741	50.0000
P_{G8}(MW)	32.6052	35.0000	31.7927	33.9594	10.7656	35.0000
P_{G11}(MW)	15.6309	21.4682	15.8564	19.2115	10.4091	30.0000
P_{G13}(MW)	16.4559	18.6308	17.8631	19.2282	12.0000	40.0000
V_{G1}(p.u.)	1.0993	1.0576	1.0984	1.0848	1.1000	1.0861
V_{G2}(p.u.)	1.0835	1.0460	1.0858	1.0684	1.0778	1.0717
V_{G5}(p.u.)	1.0412	1.0201	1.0502	1.0596	1.0595	1.0231
V_{G8}(p.u.)	1.0797	1.0339	1.0631	1.0658	1.0609	1.0358
V_{G11}(p.u.)	1.0907	1.0927	1.0564	1.0064	1.0470	1.0712
V_{G13}(p.u.)	1.0685	1.0926	1.0363	1.0495	1.0905	0.9897
T_{11}(p.u.)	1.0168	0.9929	1.0319	1.0801	1.0711	1.0383
T_{12}(p.u.)	1.1000	0.9125	1.0215	0.9675	0.9675	0.9431
T_{15}(p.u.)	1.1000	0.9551	1.0002	1.1000	1.0639	1.0266
T_{36}(p.u.)	1.0312	0.9619	0.9963	1.0374	1.0134	0.9418
Q_{C10}(p.u.)	0.0428	0.0368	0.0234	0.0472	0.0470	0.0394
Q_{C12}(p.u.)	0.0123	0.0362	0.0033	0.0071	0.0182	0.0003
Q_{C15}(p.u.)	0.0082	0.0313	0.0348	0.0057	0.0098	0.0120
Q_{C17}(p.u.)	0.0000	0.0208	0.0428	0.0083	0.0152	0.0138
Q_{C20}(p.u.)	0.0453	0.0189	0.0235	0.0500	0.0389	0.0348
Q_{C21}(p.u.)	0.0243	0.0330	0.0325	0.0493	0.0500	0.0478
Q_{C23}(p.u.)	0.0500	0.0478	0.0110	0.0379	0.0500	0.0390
Q_{C24}(p.u.)	0.0500	0.0098	0.0372	0.0448	0.0299	0.0456
Q_{C29}(p.u.)	0.0021	0.0466	0.0145	0.0477	0.0367	0.0406
F_{cost} with v-p($/h)	862.2820	861.7320	**854.3882**	**855.5369**	**831.6332**	1023.2904
Emission(ton/h)	0.2598	0.2537	**0.2598**	**0.2585**	0.3727	**0.1944**

1) CASE9 CONSIDERING BASIC FUEL COST AND EMISSION SIMULTANEOUSLY

In *CASE9*, two competing objectives of F_c and F_e are optimized at the same time. The obtained PFs are shown in Figure 16. Additionally, Table 16 gives the control variables of BC solutions.

In detail, the BC solution obtained by NHBA algorithm includes 60694.5466 $/h of F_c and 2.6445 ton/h of F_e. The BC solution achieved by NHBA-CPFD algorithm includes 60402.7420 $/h of F_c and 2.5274 ton/h of F_e.

2) CASE10 CONSIDERING BASIC FUEL COST AND ACTIVE POWER LOSS SIMULTANEOUSLY

In *CASE10*, the F_c and F_p are optimized concurrently and the obtained PFs are shown in Figure 17. The control variables of BC solutions achieved by NHBA and NHBA-CPFD

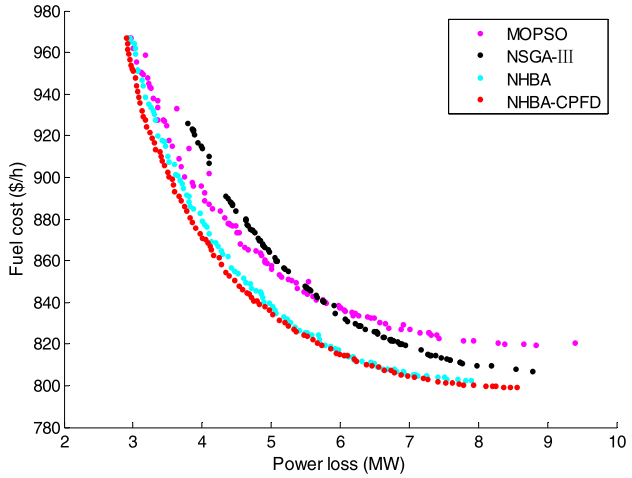

FIGURE 9. PFs obtained by different algorithms for *CASE2*.

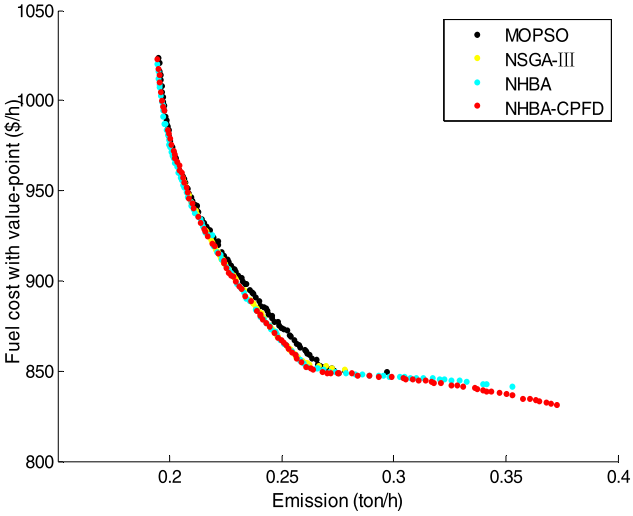

FIGURE 10. PFs obtained by different algorithms for *CASE3*.

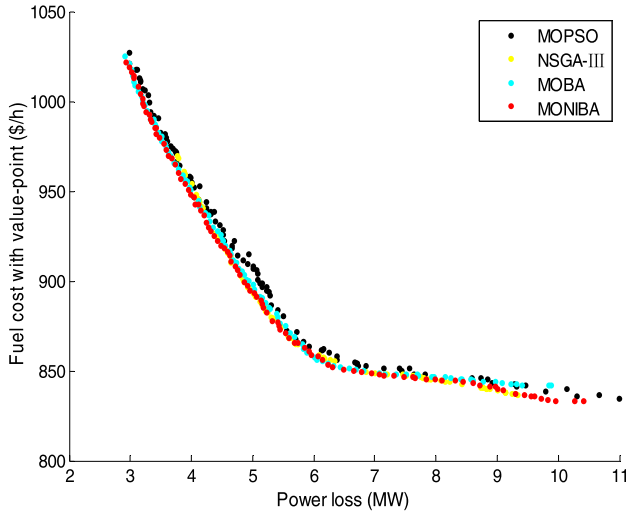

FIGURE 11. PFs obtained by different algorithms for *CASE4*.

algorithms, in contrast to the results achieved by MOPSO and NSGA-III methods, are listed in Table 17. In detail, the BC solution achieved by NHBA algorithm includes

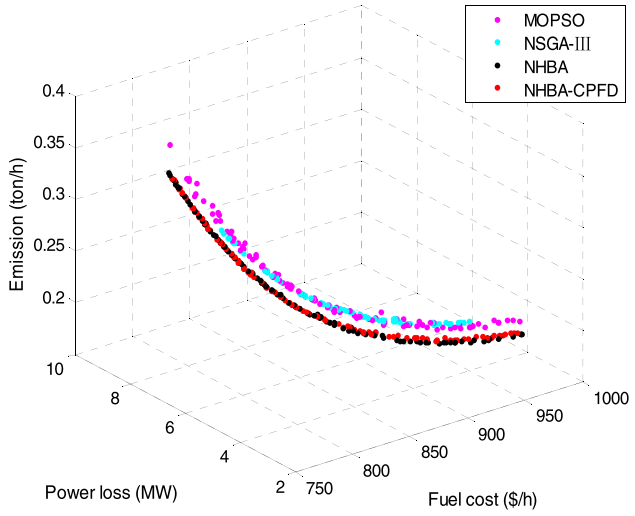

FIGURE 12. PFs obtained by different algorithms for *CASE5*.

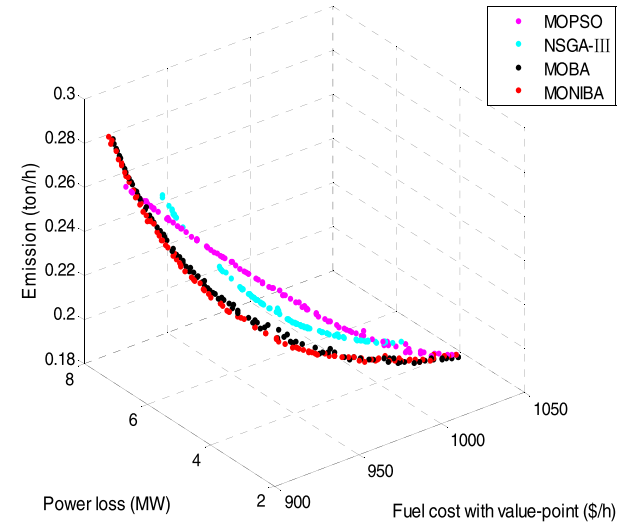

FIGURE 13. PFs obtained by different algorithms for *CASE6*.

59984.8963 \$/h of F_c and 55.1909 MW of F_p. The BC solution achieved by NHBA-CPFD algorithm includes 59589.2455 \$/h of F_c and 55.0038 MW of F_p.

VI. PERFORMANCE EVALUATION

To evaluate the distribution and diversity of POS obtained by different methods, the GD and HV metrics are adopted in this paper.

A. GD

The detailed characterization of GD index can be found in [19], [42], [43] and the formula of GD is shown as (46). For MOOPF problems, the GD index is used to measure the distance between the real PF and the obtained one. Generally speaking, the closer to zero GD index is, the PF which is more in conformity with the real one can be achieved.

$$GD = \sqrt{\sum_{i=1}^{n} de_i^2}/N_a \tag{46}$$

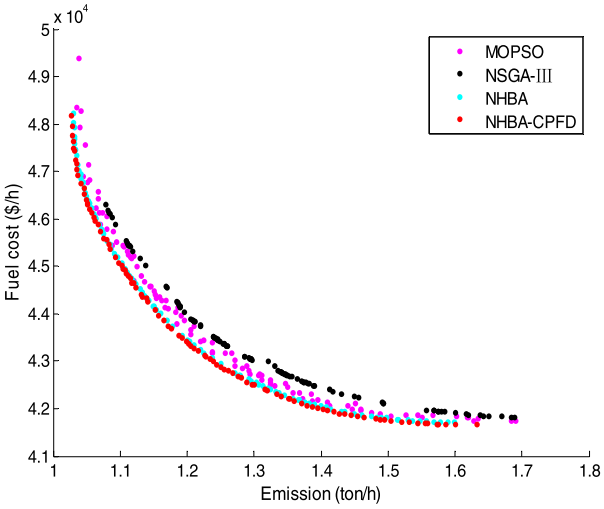

FIGURE 14. PFs obtained by different algorithms for *CASE7*.

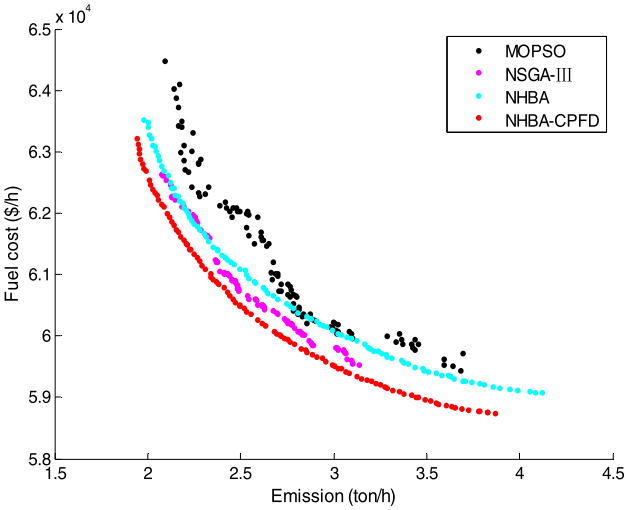

FIGURE 16. PFs obtained by different algorithms for *CASE9*.

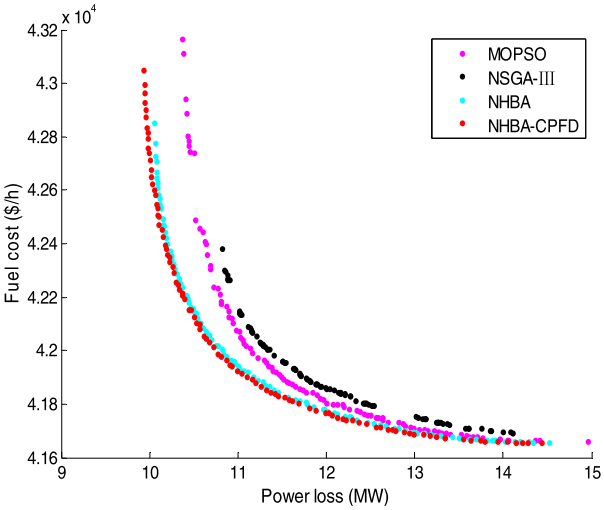

FIGURE 15. PFs obtained by different algorithms for *CASE8*.

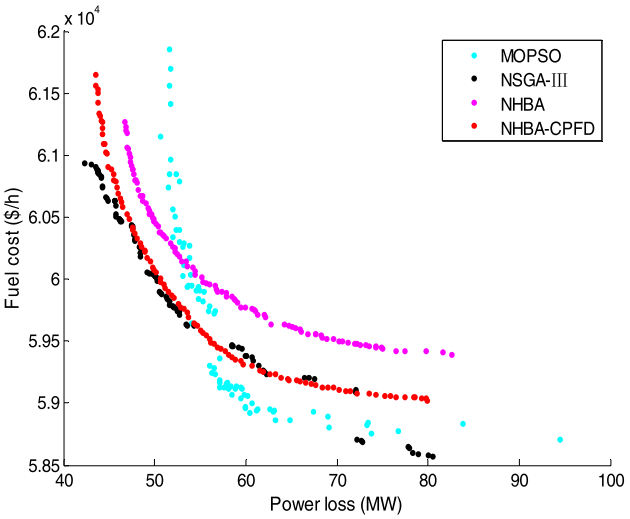

FIGURE 17. PFs obtained by different algorithms for *CASE10*.

where de_i represents the Euclidean distance between each solution of obtained POS and the nearest one in the real PF.

The POS of six testing cases on the IEEE 30-node system are analyzed by GD index. The boxplots of *CASE1*∼*CASE6* are shown in Figure 18.

Boxplot, a statistical tool to describe the dispersion of data, can visually display the maximum, minimum, median, upper and lower quartile, even outliers of a dataset. For MOOPF problems, the closer boxplots and fewer outliers mean the better convergence to the real PF.

Furthermore, Table 18 shows the mean and standard deviation of GD index for *CASE1*∼*CASE3* while Table 19 shows the mean and standard deviation of GD index for *CASE4*∼*CASE6*.

Figure 18 clearly shows that the NHBA-CPFD algorithm achieves closer boxplots and fewer outliers in all six cases on the IEEE 30-node system. In contrast to the typical MOPSO and NSGA-III algorithms, the NHBA algorithm can obtain superior POS in most cases (*CASE1*∼*CASE2*and *CASE5*∼*CASE6*). Furthermore, Table 18 and Table 19 quantitatively demonstrate that the NHBA-CPFD algorithm can obtain the smallest mean and deviation of GD index compared with other three methods.

In summary, the NHBA-CPFD algorithm is able to achieve the stable operation and it can find a uniformly distributed PF which is better consistent with the real one. In Addition, the NHBA algorithm performs well in GD index for most cases except *CASE3* and *CASE4*. The effectiveness and superiority of presented NHBA-CPFD algorithm can be verified powerfully by the computer graphics technology and dataset analysis.

B. HV

The HV index can be described as (47) [19], [42]. For MOOPF problems, the HV index represents the volume

TABLE 11. Specific solutions and control variables of CASE4.

control variables	MOPSO	NSGA-III	NHBA	NHBA-CPFD	*C4.Fv*	*C4.P*
P_{G2}(MW)	50.0929	43.1222	52.3984	47.1580	41.7416	79.8105
P_{G5}(MW)	32.6432	30.9247	31.9677	31.1918	17.6358	49.6358
P_{G8}(MW)	35.0000	34.9731	34.6347	34.8780	14.5270	35.0000
P_{G11}(MW)	24.0127	26.2895	19.6335	27.1173	10.2522	30.0000
P_{G13}(MW)	15.4112	18.9959	20.2407	15.0551	12.0000	38.5822
V_{G1}(p.u.)	1.0971	1.0992	1.0992	1.1000	1.1000	1.1000
V_{G2}(p.u.)	1.0815	1.0841	1.0922	1.0867	1.0786	1.0959
V_{G5}(p.u.)	1.0654	1.0559	1.0697	1.0666	1.0267	1.0763
V_{G8}(p.u.)	1.0673	1.0657	1.0804	1.0745	1.0609	1.0805
V_{G11}(p.u.)	1.0784	1.0749	1.0972	1.0856	1.0309	1.0979
V_{G13}(p.u.)	1.1000	1.0955	1.0707	1.0883	1.0676	1.1000
T_{11}(p.u.)	1.0824	0.9480	1.0257	0.9950	0.9911	0.9990
T_{12}(p.u.)	0.9031	0.9904	0.9754	0.9497	0.9807	0.9520
T_{15}(p.u.)	0.9807	1.0182	0.9818	1.0220	1.0321	0.9906
T_{36}(p.u.)	0.9876	0.9741	0.9868	0.9774	0.9670	0.9765
Q_{C10}(p.u.)	0.0500	0.0120	0.0276	0.0344	0.0260	0.0197
Q_{C12}(p.u.)	0.0363	0.0281	0.0277	0.0398	0.0170	0.0473
Q_{C15}(p.u.)	0.0367	0.0498	0.0242	0.0459	0.0085	0.0353
Q_{C17}(p.u.)	0.0144	0.0470	0.0256	0.0098	0.0414	0.0197
Q_{C20}(p.u.)	0.0194	0.0480	0.0397	0.0413	0.0036	0.0500
Q_{C21}(p.u.)	0.0422	0.0483	0.0310	0.0054	0.0456	0.0322
Q_{C23}(p.u.)	0.0099	0.0361	0.0315	0.0085	0.0490	0.0158
Q_{C24}(p.u.)	0.0370	0.0078	0.0269	0.0416	0.0229	0.0444
Q_{C29}(p.u.)	0.0267	0.0375	0.0205	0.0303	0.0120	0.0184
F_{cost} with v-p($/h)	868.1006	865.9864	**868.9526**	**865.9106**	**833.3204**	1022.0654
Power loss (MW)	5.6962	5.6847	**5.6761**	**5.6726**	10.4024	**2.9227**

TABLE 12. Specific solutions and control variables of CASE5.

control variables	MOPSO	NSGA-III	NHBA	NHBA-CPFD	*C5.F*	*C5.E*	*C5.P*	MOEA/D [18]
P_{G2}(MW)	57.8898	61.1591	66.8699	62.5608	49.4783	73.5913	80.0000	59.93
P_{G5}(MW)	36.2905	41.2353	36.8331	35.4638	21.0250	50.0000	50.0000	44.22
P_{G8}(MW)	35.0000	34.6782	34.2827	35.0000	21.5292	35.0000	35.0000	35.00
P_{G11}(MW)	29.2712	30.0000	27.6650	28.9848	13.1851	30.0000	30.0000	30.00
P_{G13}(MW)	40.0000	39.1884	30.2493	31.6893	12.0000	40.0000	40.0000	37.36
V_{G1}(p.u.)	1.0985	1.0472	1.0987	1.1000	1.1000	1.0942	1.1000	1.1000
V_{G2}(p.u.)	1.0869	1.0378	1.0947	1.0915	1.0891	1.0910	1.1000	1.0949
V_{G5}(p.u.)	1.0625	1.0068	1.0634	1.0671	1.0643	1.0784	1.0818	1.0786
V_{G8}(p.u.)	1.0767	1.0213	1.0815	1.0790	1.0687	1.0778	1.0849	1.0855
V_{G11}(p.u.)	1.0857	1.0523	1.0925	1.0254	1.0902	1.0456	1.0461	1.1000
V_{G13}(p.u.)	1.0386	1.0173	1.0986	1.0186	1.1000	1.0409	1.0580	1.0997
T_{11}(p.u.)	1.0861	1.0036	0.9906	1.0544	0.9796	1.0747	1.0411	1.0715
T_{12}(p.u.)	0.9933	0.9679	0.9718	0.9829	1.0061	1.0141	1.0133	0.9000
T_{15}(p.u.)	1.0515	0.9689	0.9868	1.0202	1.0164	1.0628	1.0777	0.9913
T_{36}(p.u.)	1.0770	0.9593	0.9750	1.0180	0.9714	0.9909	1.0176	0.9706
Q_{C10}(p.u.)	0.0140	0.0214	0.0494	0.0136	0.0493	0.0175	0.0194	4.767(Mvar)
Q_{C12}(p.u.)	0.0223	0.0078	0.0358	0.0012	0.0114	0.0136	0.0088	4.594(Mvar)
Q_{C15}(p.u.)	0.0080	0.0311	0.0013	0.0478	0.0106	0.0491	0.0500	4.514(Mvar)
Q_{C17}(p.u.)	0.0249	0.0407	0.0427	0.0437	0.0276	0.0350	0.0345	4.348(Mvar)
Q_{C20}(p.u.)	0.0391	0.0128	0.0417	0.0210	0.0343	0.0161	0.0172	5.000(Mvar)
Q_{C21}(p.u.)	0.0272	0.0197	0.0455	0.0491	0.0120	0.0411	0.0317	4.704(Mvar)
Q_{C23}(p.u.)	0.0103	0.0078	0.0162	0.0303	0.0303	0.0132	0.0117	3.327(Mvar)
Q_{C24}(p.u.)	0.0172	0.0482	0.0346	0.0417	0.0337	0.0500	0.0416	5.000(Mvar)
Q_{C29}(p.u.)	0.0500	0.0129	0.0332	0.0248	0.0415	0.0143	0.0168	1.262(Mvar)
Fuel cost ($/h)	879.9047	898.5219	**868.7380**	**865.4229**	**799.3578**	954.7997	967.4658	902.54
Emission(ton/h)	0.2165	0.2115	**0.2111**	**0.2116**	0.3244	**0.1943**	0.1950	0.2107
Power loss(MW)	4.2179	4.1419	**4.1744**	**4.3535**	8.5443	3.1539	**3.0176**	3.4594

covered by the obtained PF in the target space. It is used to measure the distribution uniformity and population diversity of POS. In General, the larger HV criteria is, the more widely solution domain can be covered by obtained POS.

$$HV = volume\left(\bigcup_{i=1}^{N_a} V_i\right) \tag{47}$$

TABLE 13. Specific solutions and control variables of CASE6.

control variables	MOPSO	NSGA-III	NHBA	NHBA-CPFD	*C6.Fv*	*C6.P*	*C6.E*
P_{G2}(MW)	80.0000	62.6736	73.7249	76.8300	62.9980	80.0000	71.7231
P_{G5}(MW)	50.0000	37.1759	38.0811	34.6788	21.1259	50.0000	50.0000
P_{G8}(MW)	35.0000	34.9864	34.6799	35.0000	32.8776	35.0000	35.0000
P_{G11}(MW)	24.8476	29.5603	26.3694	30.0000	10.7541	30.0000	30.0000
P_{G13}(MW)	19.1432	31.6427	34.7879	33.8819	12.0869	40.0000	40.0000
V_{G1}(p.u.)	1.1000	1.0994	1.0964	1.1000	1.0987	1.1000	1.1000
V_{G2}(p.u.)	1.1000	1.0900	1.0916	1.0936	1.0873	1.0998	1.0940
V_{G5}(p.u.)	1.1000	1.0761	1.0774	1.0605	1.0613	1.0811	1.0833
V_{G8}(p.u.)	1.0719	1.0811	1.0835	1.0762	1.0723	1.0862	1.0623
V_{G11}(p.u.)	1.1000	1.0849	1.0953	1.0531	1.0728	1.0968	1.0767
V_{G13}(p.u.)	1.0897	1.0847	1.0924	1.0931	1.0477	1.1000	1.0796
T_{11}(p.u.)	1.0433	1.0002	0.9809	1.0214	1.0657	1.0430	1.0796
T_{12}(p.u.)	0.9936	0.9907	1.0111	0.9455	0.9983	0.9000	0.9165
T_{15}(p.u.)	0.9903	1.0118	0.9965	1.0391	1.0587	0.9773	1.0013
T_{36}(p.u.)	1.0368	0.9905	0.9838	0.9883	1.0404	0.9991	1.0044
Q_{C10}(p.u.)	0.0175	0.0089	0.0405	0.0325	0.0180	0.0367	0.0228
Q_{C12}(p.u.)	0.0473	0.0221	0.0447	0.0025	0.0084	0.0426	0.0486
Q_{C15}(p.u.)	0.0500	0.0271	0.0089	0.0357	0.0274	0.0420	0.0413
Q_{C17}(p.u.)	0.0000	0.0394	0.0264	0.0318	0.0078	0.0407	0.0425
Q_{C20}(p.u.)	0.0500	0.0083	0.0366	0.0233	0.0451	0.0216	0.0214
Q_{C21}(p.u.)	0.0500	0.0211	0.0492	0.0422	0.0365	0.0093	0.0145
Q_{C23}(p.u.)	0.0500	0.0269	0.0365	0.0188	0.0107	0.0244	0.0408
Q_{C24}(p.u.)	0.0454	0.0177	0.0205	0.0420	0.0500	0.0082	0.0178
Q_{C29}(p.u.)	0.0500	0.0311	0.0157	0.0446	0.0300	0.0134	0.0211
F_{cost} with v-p($/h)	982.4655	971.7659	**964.8493**	**962.8123**	**904.6377**	1026.9732	1019.6235
Power loss(MW)	3.9754	4.1318	**3.9018**	**3.9637**	7.4745	**2.9541**	3.2668
Emission(ton/h)	0.2093	0.2095	**0.2047**	**0.2041**	0.2869	0.1949	**0.1943**

TABLE 14. Specific solutions and control variables of CASE7.

control variables	MOPSO	NSGA-III	NHBA	NHBA-CPFD	*C7.E*	*C7.F*
P_{G2}(MW)	97.5669	99.7273	99.4683	99.9912	100.0000	100.0000
P_{G3}(MW)	96.8167	90.1018	91.7357	95.9130	140.0000	41.4411
P_{G6}(MW)	99.0831	99.7778	99.9067	99.7928	100.0000	94.9631
P_{G8}(MW)	324.9300	338.9631	353.2901	357.0414	271.7851	437.9550
P_{G9}(MW)	99.0032	99.9404	100.0000	99.7146	100.0000	94.4472
P_{G12}(MW)	325.6119	312.1681	298.7424	296.4971	237.6294	358.9421
V_{G1}(p.u.)	1.1000	1.0693	1.0989	1.0999	1.1000	1.1000
V_{G2}(p.u.)	1.1000	1.0586	1.0957	1.1000	1.1000	1.0999
V_{G3}(p.u.)	1.1000	1.0373	1.0942	1.1000	1.1000	1.1000
V_{G6}(p.u.)	1.1000	1.0462	1.0986	1.0999	1.1000	1.1000
V_{G8}(p.u.)	1.1000	1.0431	1.0995	1.0999	1.1000	1.1000
V_{G9}(p.u.)	1.1000	1.0260	1.0994	1.1000	1.1000	1.1000
V_{G12}(p.u.)	1.1000	1.0291	1.0991	1.0998	1.1000	1.0962
T_{19}(p.u.)	1.0462	0.9110	1.0977	0.9645	0.9691	0.9614
T_{20}(p.u.)	1.0382	1.0976	1.0234	1.0065	0.9890	1.0244
T_{31}(p.u.)	1.0307	0.9180	1.0882	1.0022	1.0140	0.9866
T_{35}(p.u.)	1.0905	0.9739	0.9485	1.0190	1.0623	0.9738
T_{36}(p.u.)	1.0925	0.9237	1.0853	1.0185	0.9984	1.0451
T_{37}(p.u.)	1.0664	1.0210	1.0399	1.0142	1.0638	0.9888
T_{41}(p.u.)	1.0223	1.0350	1.0509	0.9919	1.0096	0.9936
T_{46}(p.u.)	0.9431	1.0072	1.0440	1.0021	1.0298	0.9748
T_{54}(p.u.)	0.9878	0.9599	1.0997	1.0646	1.0852	1.0535
T_{58}(p.u.)	1.0296	0.9466	1.0449	1.0081	0.9990	1.0165
T_{59}(p.u.)	1.0566	0.9294	0.9650	1.0099	1.0010	1.0132
T_{65}(p.u.)	1.0353	0.9290	1.0109	1.0184	1.0213	1.0181
T_{66}(p.u.)	1.0406	0.9149	0.9932	1.0237	1.0235	1.0304
T_{71}(p.u.)	1.0978	0.9628	0.9744	1.0020	1.0060	1.0041
T_{73}(p.u.)	1.0935	0.9929	1.0665	1.0094	1.0419	0.9884
T_{76}(p.u.)	0.9227	1.0470	1.0662	0.9279	0.9207	0.9312
T_{80}(p.u.)	1.0964	0.9798	1.0998	1.0012	1.0037	1.0077
Q_{C18}(p.u.)	0.0558	0.0514	0.2998	0.0473	0.0399	0.0544
Q_{C25}(p.u.)	0.1671	0.1190	0.2006	0.1120	0.1129	0.1293
Q_{C53}(p.u.)	0.1893	0.1092	0.1314	0.1523	0.1464	0.1793
Emission(ton/h)	1.2236	1.2592	**1.2192**	**1.2164**	**1.0271**	1.6319
Fuel cost($/h)	43458.9119	43323.7670	**43244.5741**	**43221.5876**	48186.3156	**41678.6457**

TABLE 15. Specific solutions and control variables of CASE8.

control variables	MOPSO	NSGA-III	NHBA	NHBA-CPFD	*C8.P*	*C8.F*
P_{G2}(MW)	87.5514	74.0796	54.4425	71.7354	34.5143	95.4736
P_{G3}(MW)	60.0672	55.9676	60.4878	58.7146	91.6050	45.0297
P_{G6}(MW)	90.8522	94.8605	74.2930	80.8100	94.5210	73.2305
P_{G8}(MW)	369.5724	376.8044	400.8033	390.0261	329.4453	455.9718
P_{G9}(MW)	99.9100	99.9678	99.8446	100.0000	100.0000	91.7225
P_{G12}(MW)	410.0000	409.2794	410.0000	410.0000	410.0000	360.7749
V_{G1}(p.u.)	1.1000	1.0263	1.0993	1.0996	1.0996	1.0967
V_{G2}(p.u.)	1.1000	1.0225	1.0955	1.0972	1.0960	1.0948
V_{G3}(p.u.)	1.1000	1.0208	1.0912	1.0938	1.0966	1.0881
V_{G6}(p.u.)	1.1000	1.0276	1.0965	1.1000	1.1000	1.0858
V_{G8}(p.u.)	1.1000	1.0360	1.0992	1.0997	1.1000	1.0929
V_{G9}(p.u.)	1.1000	1.0278	1.0877	1.0890	1.0864	1.0818
V_{G12}(p.u.)	1.1000	1.0198	1.0818	1.0911	1.0883	1.0750
T_{19}(p.u.)	0.9744	1.0409	1.0570	1.0170	0.9657	1.0455
T_{20}(p.u.)	1.0075	0.9002	0.9806	1.0584	1.0043	1.0315
T_{31}(p.u.)	0.9741	1.0219	0.9741	1.0230	1.0638	0.9807
T_{35}(p.u.)	1.0822	0.9909	1.0983	1.0548	1.0597	1.0736
T_{36}(p.u.)	1.0645	1.0362	0.9921	0.9568	0.9911	0.9471
T_{37}(p.u.)	0.9864	0.9947	1.0641	0.9723	0.9819	0.9664
T_{41}(p.u.)	1.0035	0.9339	1.0337	0.9947	0.9922	0.9811
T_{46}(p.u.)	0.9756	0.9540	0.9684	1.0307	1.0226	1.0263
T_{54}(p.u.)	0.9530	0.9326	0.9707	0.9453	0.9512	0.9369
T_{58}(p.u.)	1.0267	0.9226	0.9805	1.0043	0.9893	1.0118
T_{59}(p.u.)	1.0293	0.9214	0.9580	0.9855	1.0071	0.9724
T_{65}(p.u.)	1.1000	0.9330	0.9747	0.9821	1.0050	0.9612
T_{66}(p.u.)	1.0217	0.9000	0.9416	0.9584	0.9621	0.9543
T_{71}(p.u.)	0.9885	0.9058	0.9845	0.9679	0.9672	0.9624
T_{73}(p.u.)	0.9638	1.0078	0.9431	1.0178	0.9859	1.0268
T_{76}(p.u.)	0.9496	0.9735	1.0493	1.0745	1.0717	1.0581
T_{80}(p.u.)	1.0145	0.9391	1.0135	0.9958	0.9822	1.0010
Q_{C18}(p.u.)	0.0340	0.1298	0.1670	0.1054	0.0759	0.1205
Q_{C25}(p.u.)	0.1822	0.1462	0.1508	0.1756	0.1861	0.1605
Q_{C53}(p.u.)	0.0945	0.1374	0.1748	0.1065	0.0825	0.0812
Power loss(MW)	11.0649	11.4066	**11.0174**	**10.9884**	**9.9299**	14.4357
Fuel cost($/h)	42029.0946	41983.5570	**41934.2468**	**41925.5743**	43052.0891	**41655.1128**

where $V_i$indicates the volume formed by the ith solution and reference points.

The boxplots of HV index for *CASE1*∼*CASE6* are shown in Figure 19. Meanwhile, Table 20 gives the mean and standard deviation of HV index for *CASE1*∼*CASE3* while Table 21 gives the details of HV index for *CASE4*∼*CASE6*.

It clearly shows that the NHBA and NHBA-CPFD algorithms can achieve larger value of HV index in bi-objective cases on the IEEE 30-node system after eliminating the MOPSO algorithm with many outliers.

However, there is a slight insufficiency that the tri-objective optimization cases are not doing well in HV index. Figure 19 shows that compared with MOPSO and NSGA-III methods, the NHBA and NHBA-CPFD algorithms can achieve closer boxplots in most cases on the IEEE 30-node system. The smaller deviations of NHBA and NHBA-CPFD shown on Table 20 and Table 21 effectively illustrate the stability operation of NHBA and NHBA-CPFD algorithms.

C. DOMINANCE RATE OF BC SOLUTIONS

Based on the experimental results shown in Section 5, MOPSO and NSGA-III algorithms can obtain well-distributed PFs only in the small-scale IEEE 30-node system while NHBA and NHBA-CPFD algorithms can achieve uniform-distributed PFs even in the large-scale systems.

In more detail, Table 22 shows the dominant relationships between the BC solutions obtained by the NHBA-CPFD algorithm and the ones obtained by the other three algorithms.

The *U-R* of Table 22 represents that the two BC solutions do not dominate each other based on the objective values. Table 22 intuitively indicates that the BC solutions of the NHBA-CPFD algorithm have the 80% probability to dominate MOPSO algorithm and the 60% probability to dominate NSGA-III and NHBA algorithms. In particular, it is worthy to mention that for the four cases (*CASE7*∼*CASE10*) which are carried out on the IEEE 57-node or IEEE 118-node systems,

TABLE 16. Specific solutions and control variables of CASE9.

control variables	MOPSO	NSGA-III	NHBA	NHBA-CPFD	control variables	MOPSO	NSGA-III	NHBA	NHBA-CPFD
P_{G4}(MW)	15.8872	24.2017	18.2941	5.2108	V_{G26}(p.u.)	1.0218	1.0754	0.9868	0.9788
P_{G6}(MW)	6.8991	16.8434	21.4065	7.6500	V_{G27}(p.u.)	1.0145	1.0509	0.9836	1.0190
P_{G8}(MW)	8.8348	7.3094	15.8496	8.4912	V_{G31}(p.u.)	1.0375	1.0794	0.9864	1.0095
P_{G10}(MW)	216.4285	278.5921	207.1529	236.56717	V_{G32}(p.u.)	0.9814	0.9869	1.0013	1.0368
P_{G12}(MW)	251.5344	150.0178	198.4023	188.9828	V_{G34}(p.u.)	0.9641	0.9975	1.0147	1.0293
P_{G15}(MW)	20.7546	24.2361	22.4010	18.1767	V_{G36}(p.u.)	0.9599	1.0544	1.0052	1.0329
P_{G18}(MW)	25.0000	55.6633	30.4001	65.1160	V_{G40}(p.u.)	0.9800	1.0831	1.0412	1.0209
P_{G19}(MW)	5.1272	5.7621	8.9978	5.4255	V_{G42}(p.u.)	1.0320	0.9911	1.0182	1.0320
P_{G24}(MW)	6.5516	10.0953	8.7019	11.0393	V_{G46}(p.u.)	1.0494	1.0366	1.0003	1.0133
P_{G25}(MW)	107.6419	100.861	100.7158	100.0390	V_{G49}(p.u.)	1.0476	0.9864	0.9968	1.0050
P_{G26}(MW)	107.8829	100.0000	111.4576	103.0140	V_{G54}(p.u.)	1.0816	0.9813	0.9870	0.9906
P_{G27}(MW)	12.5823	13.2068	12.2746	8.5944	V_{G55}(p.u.)	1.0571	0.9905	0.9894	0.9923
P_{G31}(MW)	18.1318	10.7255	9.9998	20.3871	V_{G56}(p.u.)	1.0762	0.9913	1.0222	0.9883
P_{G32}(MW)	52.3239	47.5384	55.1529	42.3822	V_{G59}(p.u.)	0.9915	1.0601	1.0018	1.0131
P_{G34}(MW)	14.5950	21.8714	15.6786	14.4781	V_{G61}(p.u.)	1.0908	1.0497	0.9997	1.0022
P_{G36}(MW)	42.1874	25.0000	25.2626	25.0000	V_{G62}(p.u.)	1.0144	0.9759	1.0078	1.0166
P_{G40}(MW)	9.7413	12.7501	11.6654	9.4283	V_{G65}(p.u.)	1.0752	1.0260	0.9964	0.9912
P_{G42}(MW)	9.7946	12.0613	9.0105	8.1586	V_{G66}(p.u.)	1.0194	0.9750	1.0041	1.0348
P_{G46}(MW)	30.5225	48.9436	74.7918	50.8135	V_{G69}(p.u.)	1.0225	0.9453	0.9787	1.0122
P_{G49}(MW)	197.8519	250.0000	219.8476	223.6021	V_{G70}(p.u.)	1.0160	1.0490	1.0348	1.0321
P_{G54}(MW)	204.8801	146.9598	142.0671	148.1755	V_{G72}(p.u.)	1.0298	1.0603	1.0019	0.9868
P_{G55}(MW)	25.4822	27.2273	44.7841	32.3898	V_{G73}(p.u.)	0.9750	0.9751	0.9806	0.9889
P_{G56}(MW)	26.9217	25.1975	27.5473	39.1927	V_{G74}(p.u.)	0.9749	0.9437	1.0006	0.9825
P_{G59}(MW)	50.0000	94.5396	56.3647	54.6768	V_{G76}(p.u.)	1.0512	1.0302	1.0087	1.0322
P_{G61}(MW)	154.9293	140.7908	139.2697	125.0486	V_{G77}(p.u.)	1.0877	1.0403	1.0109	1.0284
P_{G62}(MW)	57.9668	40.1860	50.2893	77.2332	V_{G80}(p.u.)	1.0795	1.0140	1.0116	1.0258
P_{G65}(MW)	352.5528	406.9774	398.3242	416.8112	V_{G85}(p.u.)	0.9589	0.9932	0.9964	0.9782
P_{G66}(MW)	247.2315	202.4889	275.0035	254.0173	V_{G87}(p.u.)	0.9787	1.0352	0.9671	0.9937
P_{G69}(MW)	35.5373	40.7117	42.5779	30.0000	V_{G89}(p.u.)	1.0481	0.9996	1.0140	1.0327
P_{G70}(MW)	10.0351	10.0133	22.8390	21.0943	V_{G90}(p.u.)	1.0345	1.0211	1.0118	0.9959
P_{G72}(MW)	8.7784	5.5414	12.5439	7.3244	V_{G91}(p.u.)	1.0972	0.9712	0.9935	1.0075
P_{G73}(MW)	5.8829	5.8237	5.3950	8.8796	V_{G92}(p.u.)	1.0576	1.0204	0.9890	1.0243
P_{G74}(MW)	74.7998	30.6864	30.8662	28.0854	V_{G99}(p.u.)	1.0945	1.0937	0.9811	1.0296
P_{G76}(MW)	36.0810	25.9036	29.4534	34.9853	V_{G100}(p.u.)	0.9945	1.0234	1.0208	1.0362
P_{G77}(MW)	166.3017	166.3802	175.6678	211.7833	V_{G103}(p.u.)	1.0169	1.0538	0.9853	1.0013
P_{G80}(MW)	40.4215	25.8462	33.6241	58.2015	V_{G104}(p.u.)	1.0085	1.0169	0.9929	1.0111
P_{G85}(MW)	10.1321	10.1511	12.9354	21.2169	V_{G105}(p.u.)	0.9967	1.0023	1.0143	1.0084
P_{G87}(MW)	173.5865	227.9653	170.5792	161.4976	V_{G107}(p.u.)	1.0768	1.0012	1.0416	1.0000
P_{G89}(MW)	177.3745	73.3096	69.4068	75.4951	V_{G110}(p.u.)	1.0622	1.0093	0.9770	1.0198
P_{G90}(MW)	16.4651	9.8098	8.6340	10.5362	V_{G111}(p.u.)	1.0998	1.0129	0.9985	1.0196
P_{G91}(MW)	46.1355	29.0455	38.4998	30.0587	V_{G112}(p.u.)	1.0425	1.0280	0.9722	1.0208
P_{G92}(MW)	121.7730	137.3909	163.4723	139.7410	V_{G113}(p.u.)	1.0904	1.0215	1.0020	1.0192
P_{G99}(MW)	205.5028	146.57345	125.1281	120.6078	V_{G116}(p.u.)	1.0527	0.9841	1.0060	1.0557
P_{G100}(MW)	114.6704	172.8365	152.7393	192.6256	T_{8}(p.u.)	1.0159	1.0169	1.0796	0.9604
P_{G103}(MW)	8.0627	13.2622	10.2447	11.4028	T_{32}(p.u.)	1.0738	1.0030	1.0509	1.0021
P_{G104}(MW)	30.7767	30.9723	44.3370	29.4859	T_{36}(p.u.)	1.0325	0.9152	0.9199	0.9932
P_{G105}(MW)	25.0000	41.4724	62.1228	33.0573	T_{51}(p.u.)	0.9577	0.9923	0.9607	0.9414
P_{G107}(MW)	9.4323	12.8313	16.1199	14.1175	T_{93}(p.u.)	0.9092	0.9141	0.9230	0.9678
P_{G110}(MW)	25.2439	25.1653	38.7978	33.5484	T_{95}(p.u.)	1.0809	1.0085	1.0833	1.0148
P_{G111}(MW)	26.0875	64.6183	36.3168	37.6015	T_{102}(p.u.)	1.0057	1.0483	1.0206	0.9220
P_{G112}(MW)	25.9478	42.2265	43.7880	32.5831	T_{107}(p.u.)	1.0462	1.0878	1.0759	0.9021
P_{G113}(MW)	49.0916	95.8758	38.1490	52.3459	T_{127}(p.u.)	0.9101	0.9674	1.0441	1.0273
P_{G116}(MW)	29.3181	29.7723	39.1324	36.6298	Q_{C34}(p.u.)	0.0447	0.2100	0.1339	0.1358
V_{G1}(p.u.)	1.0273	0.9871	1.0073	1.0081	Q_{C44}(p.u.)	0.0792	0.1783	0.1325	0.0697
V_{G4}(p.u.)	1.0726	0.9828	0.9915	1.0267	Q_{C45}(p.u.)	0.2838	0.2978	0.2846	0.1274
V_{G6}(p.u.)	1.0230	1.0109	1.0192	0.9994	Q_{C46}(p.u.)	0.2543	0.0054	0.1164	0.2244
V_{G8}(p.u.)	1.0656	1.0348	0.9933	1.0351	Q_{C48}(p.u.)	0.0358	0.0807	0.2195	0.0517
V_{G10}(p.u.)	0.9997	1.0084	0.9881	0.9910	Q_{C74}(p.u.)	0.1011	0.1042	0.2268	0.2144
V_{G12}(p.u.)	1.0402	1.0569	0.9921	0.9849	Q_{C79}(p.u.)	0.0030	0.0782	0.0470	0.1977
V_{G15}(p.u.)	1.0693	1.0061	1.0106	1.0421	Q_{C82}(p.u.)	0.1612	0.2642	0.2484	0.0983
V_{G18}(p.u.)	1.0650	1.0522	0.9887	0.9783	Q_{C83}(p.u.)	0.1521	0.2417	0.2077	0.1310
V_{G19}(p.u.)	0.9847	0.9748	1.0158	1.0430	Q_{C105}(p.u.)	0.2851	0.0780	0.2263	0.2606
V_{G24}(p.u.)	1.0175	1.0352	0.9627	1.0526	Q_{C107}(p.u.)	0.1462	0.0973	0.1985	0.2503
V_{G25}(p.u.)	1.0102	0.9595	1.0073	0.9898	Q_{C110}(p.u.)	0.1852	0.1640	0.0401	0.0182
					Emission (ton/h)	2.7826	2.4815	**2.6445**	**2.5274**
					Fuel cost ($/h)	60423.2970	60780.8762	**60694.5466**	**60402.7420**

the BC solutions obtained by NHBA-CPFD algorithm are more superior to those obtained by NHBA algorithm. It powerfully demonstrates that when adopting the same algorithm, the proposed CPFD strategy is more advantageous than CPM method in dealing with the high-dimensional optimizations of complex systems.

TABLE 17. Specific solutions and control variables of CASE10.

control variables	MOPSO	NSGA-III	NHBA	NHBA-CPFD	control variables	MOPSO	NSGA-III	NHBA	NHBA-CPFD
P_{G4}(MW)	19.9176	5.0000	6.7934	5.1596	V_{G26}(p.u.)	1.0449	0.9895	1.0122	0.9870
P_{G6}(MW)	6.8619	22.7851	21.2749	8.3128	V_{G27}(p.u.)	1.0201	0.9609	0.9952	0.9750
P_{G8}(MW)	7.7176	7.2779	21.3673	5.3250	V_{G31}(p.u.)	1.0339	0.9647	1.0107	1.0027
P_{G10}(MW)	150.7075	186.5229	181.5324	223.7947	V_{G32}(p.u.)	1.0303	1.0110	0.9961	1.0201
P_{G12}(MW)	260.6861	234.1053	182.3484	152.6505	V_{G34}(p.u.)	1.0353	1.0121	1.0061	1.0053
P_{G15}(MW)	10.4528	12.5793	22.6105	13.0667	V_{G36}(p.u.)	1.0605	1.0005	0.9822	1.0342
P_{G18}(MW)	59.7856	46.8689	57.2657	45.7977	V_{G40}(p.u.)	1.0310	1.0029	0.9576	1.0718
P_{G19}(MW)	16.8865	21.1907	5.0637	19.5838	V_{G42}(p.u.)	1.0786	1.0358	1.0033	1.0467
P_{G24}(MW)	10.3805	8.6509	23.0570	5.0000	V_{G46}(p.u.)	1.0557	1.0185	1.0157	1.0419
P_{G25}(MW)	101.3770	127.7909	133.8328	124.2746	V_{G49}(p.u.)	1.0201	1.0061	1.0345	1.0517
P_{G26}(MW)	238.0933	218.8530	257.5043	321.1968	V_{G54}(p.u.)	1.0198	1.0029	1.0170	1.0459
P_{G27}(MW)	8.6757	12.9486	12.3010	8.1820	V_{G55}(p.u.)	1.0324	1.0008	1.0181	1.0503
P_{G31}(MW)	8.0482	21.4135	25.9497	11.8425	V_{G56}(p.u.)	1.0100	1.0195	1.0116	1.0401
P_{G32}(MW)	98.1253	50.5916	69.1772	68.6069	V_{G59}(p.u.)	1.0681	1.0258	1.0247	1.0435
P_{G34}(MW)	17.0775	8.4393	10.8604	22.2504	V_{G61}(p.u.)	1.0836	1.0104	1.0081	1.0554
P_{G36}(MW)	37.1153	69.4697	36.8194	74.4961	V_{G62}(p.u.)	1.0300	1.0289	1.0199	1.0187
P_{G40}(MW)	8.0000	9.0326	17.2059	8.2132	V_{G65}(p.u.)	1.0754	1.0118	1.0078	1.0492
P_{G42}(MW)	10.4144	21.9630	12.5103	15.0177	V_{G66}(p.u.)	1.0627	1.0595	1.0524	1.0409
P_{G46}(MW)	31.2176	53.5697	62.7834	46.5214	V_{G69}(p.u.)	1.0254	1.0453	1.0161	1.0204
P_{G49}(MW)	238.9606	164.9918	150.8057	93.7033	V_{G70}(p.u.)	1.0291	0.9785	0.9888	1.0645
P_{G54}(MW)	191.5523	216.8517	232.3273	244.9136	V_{G72}(p.u.)	1.0499	1.0294	1.0369	1.0448
P_{G55}(MW)	48.9235	56.3268	39.5023	48.6081	V_{G73}(p.u.)	1.0218	1.0504	0.9977	0.9971
P_{G56}(MW)	39.4067	81.5120	77.2177	32.6459	V_{G74}(p.u.)	0.9959	1.0164	1.0079	0.9830
P_{G59}(MW)	154.7012	121.4729	103.8788	173.4169	V_{G76}(p.u.)	1.0148	1.0271	1.0088	1.0329
P_{G61}(MW)	177.8504	199.0160	112.1634	124.3863	V_{G77}(p.u.)	1.0125	1.0354	1.0160	1.0359
P_{G62}(MW)	54.3146	26.7623	28.1174	29.3542	V_{G80}(p.u.)	1.0057	0.9943	1.0124	1.0286
P_{G65}(MW)	330.3925	258.6241	274.1791	254.5513	V_{G85}(p.u.)	0.9753	0.9887	0.9798	0.9921
P_{G66}(MW)	137.2145	201.4848	263.2416	214.6704	V_{G87}(p.u.)	0.9607	0.9780	0.9302	0.9343
P_{G69}(MW)	32.4897	57.7153	52.2267	30.4511	V_{G89}(p.u.)	1.0700	1.0065	1.0175	1.0682
P_{G70}(MW)	13.9753	10.8531	12.6945	23.5177	V_{G90}(p.u.)	1.0550	1.0050	1.0042	1.0633
P_{G72}(MW)	5.2212	13.8617	5.0520	21.0105	V_{G91}(p.u.)	1.0666	0.9979	1.0126	1.0642
P_{G73}(MW)	5.2895	6.2214	5.0288	16.3443	V_{G92}(p.u.)	1.0660	1.0104	1.0221	1.0600
P_{G74}(MW)	44.4335	30.6756	38.6052	72.2747	V_{G99}(p.u.)	1.0720	0.9772	1.0130	1.0274
P_{G76}(MW)	47.8487	65.7396	31.9824	28.9239	V_{G100}(p.u.)	1.0141	1.0034	0.9996	1.0263
P_{G77}(MW)	164.6913	160.2489	170.2171	150.9688	V_{G103}(p.u.)	0.9869	1.0035	0.9820	1.0135
P_{G80}(MW)	67.4293	27.6238	59.5682	32.9770	V_{G104}(p.u.)	0.9728	0.9992	0.9964	1.0125
P_{G85}(MW)	10.3534	15.1266	19.9493	21.9112	V_{G105}(p.u.)	0.9848	0.9919	0.9863	1.0159
P_{G87}(MW)	101.6992	157.8482	102.3793	100.0000	V_{G107}(p.u.)	0.9779	1.0006	0.9479	1.0121
P_{G89}(MW)	65.2535	67.3263	64.7034	83.3234	V_{G110}(p.u.)	1.0549	0.9753	0.9915	0.9984
P_{G90}(MW)	8.4383	9.5007	16.0758	8.0934	V_{G111}(p.u.)	1.0669	0.9486	0.9892	1.0042
P_{G91}(MW)	21.5391	28.7783	33.4298	46.7578	V_{G112}(p.u.)	1.0925	0.9800	0.9941	0.9973
P_{G92}(MW)	101.6862	102.4969	110.3340	112.5793	V_{G113}(p.u.)	1.0231	0.9911	1.0021	1.0173
P_{G99}(MW)	116.8600	101.0885	158.8755	108.4276	V_{G116}(p.u.)	1.0231	1.0136	0.9984	1.0151
P_{G100}(MW)	113.5326	100.1413	117.9367	108.3333	T_{8}(p.u.)	1.0675	0.9698	0.9678	0.9694
P_{G103}(MW)	8.5868	8.2474	8.0771	8.0925	T_{32}(p.u.)	0.9925	0.9407	1.0077	0.9768
P_{G104}(MW)	25.8162	38.9282	25.1431	29.3802	T_{36}(p.u.)	0.9085	1.0444	0.9782	1.0568
P_{G105}(MW)	25.3319	41.3443	25.7605	28.4204	T_{51}(p.u.)	0.9367	0.9569	0.9986	0.9019
P_{G107}(MW)	8.3872	8.6289	13.3849	8.1473	T_{93}(p.u.)	1.0546	0.9420	0.9399	1.0145
P_{G110}(MW)	28.4319	26.5478	36.3842	25.4490	T_{95}(p.u.)	0.9420	0.9289	1.0522	1.0081
P_{G111}(MW)	27.2072	25.3709	31.7956	25.1543	T_{102}(p.u.)	1.0546	1.0886	1.0083	1.0495
P_{G112}(MW)	25.0000	33.4043	25.3674	37.1478	T_{107}(p.u.)	1.0576	0.9398	0.9193	1.0676
P_{G113}(MW)	55.5100	27.5689	25.0092	81.3185	T_{127}(p.u.)	0.9080	1.0012	0.9635	0.9391
P_{G116}(MW)	31.1489	25.1972	38.5212	26.2355	Q_{C34}(p.u.)	0.2534	0.1113	0.2067	0.2816
V_{G1}(p.u.)	1.0137	1.0083	1.0266	1.0198	Q_{C44}(p.u.)	0.0395	0.0250	0.2177	0.2759
V_{G4}(p.u.)	1.0010	1.0027	1.0433	1.0218	Q_{C45}(p.u.)	0.0462	0.1463	0.1041	0.1006
V_{G6}(p.u.)	1.0566	0.9955	1.0047	0.9897	Q_{C46}(p.u.)	0.2900	0.2550	0.1350	0.0049
V_{G8}(p.u.)	1.0058	1.0364	0.9870	1.0149	Q_{C48}(p.u.)	0.2647	0.0055	0.1919	0.2453
V_{G10}(p.u.)	1.0018	0.9974	1.0252	1.0269	Q_{C74}(p.u.)	0.0712	0.2235	0.2734	0.1835
V_{G12}(p.u.)	0.9981	1.0062	0.9797	0.9894	Q_{C79}(p.u.)	0.2897	0.2282	0.1535	0.2978
V_{G15}(p.u.)	0.9858	1.0219	0.9946	1.0135	Q_{C82}(p.u.)	0.2652	0.0616	0.0972	0.1256
V_{G18}(p.u.)	0.9957	1.0169	0.9893	1.0045	Q_{C83}(p.u.)	0.2044	0.1659	0.1924	0.2669
V_{G19}(p.u.)	1.0367	1.0115	1.0042	1.0631	Q_{C105}(p.u.)	0.1400	0.2435	0.2533	0.2349
V_{G24}(p.u.)	1.0843	1.0285	1.0073	1.0204	Q_{C107}(p.u.)	0.2953	0.2120	0.2575	0.1333
V_{G25}(p.u.)	0.9588	1.0501	0.9858	1.0184	Q_{C110}(p.u.)	0.0629	0.1663	0.2500	0.1355
					Power loss (MW)	57.0368	58.4603	**55.1909**	**55.0038**
					Fuel cost ($/h)	59133.1054	59474.4030	**59984.8963**	**59589.2455**

D. SUPERPOSITION PFs

Each case was carried out 30 times independently. The superposition diagrams of several typical cases are represented. Hereinto, Figure 20 shows the results of four involved algorithms when dealing with a bi-objective optimization problem (*CASE1*) on IEEE 30-node system and Figure 21 gives the results of a tri-objective optimization problem (*CASE5*) on the same system. Figure 22 shows the

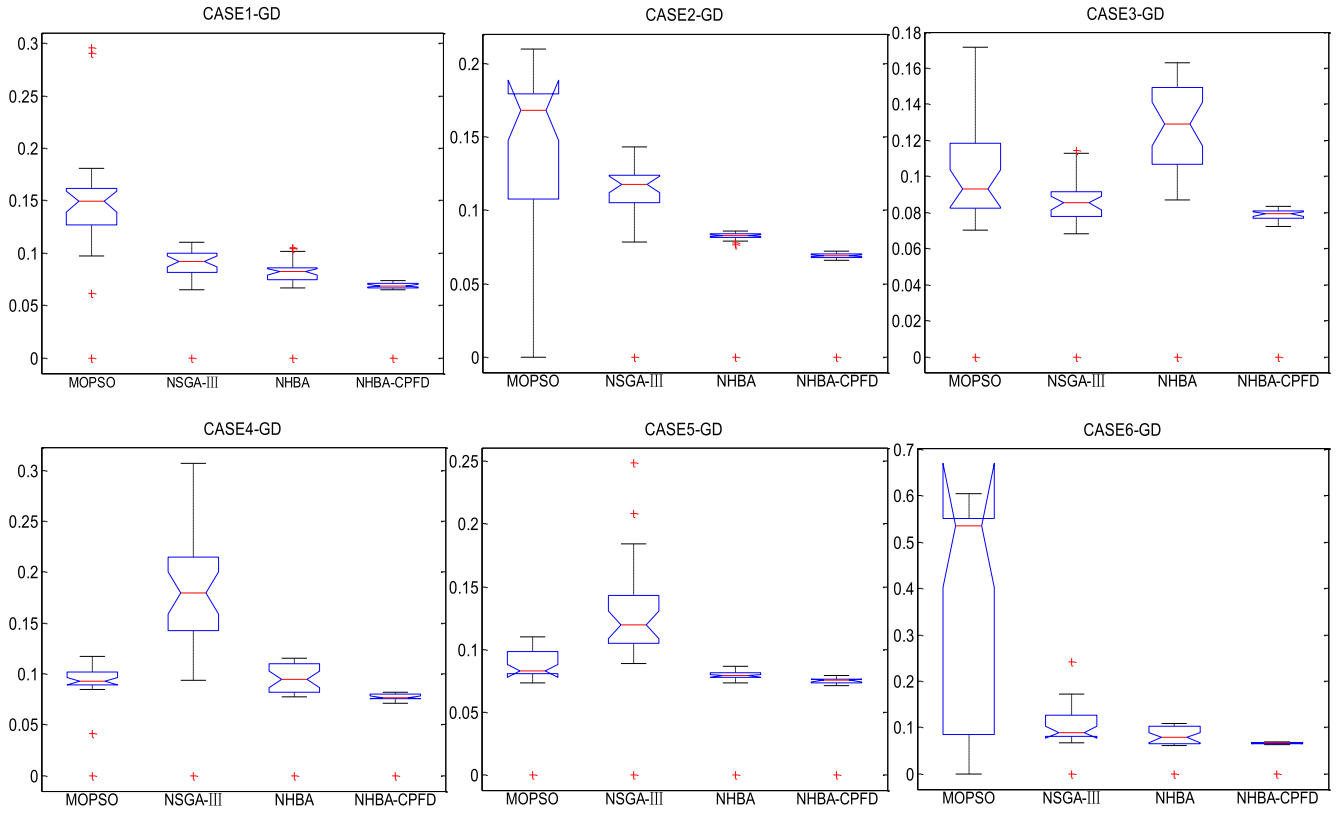

FIGURE 18. Boxplots of the GD index for *CASE1*∼*CASE6*.

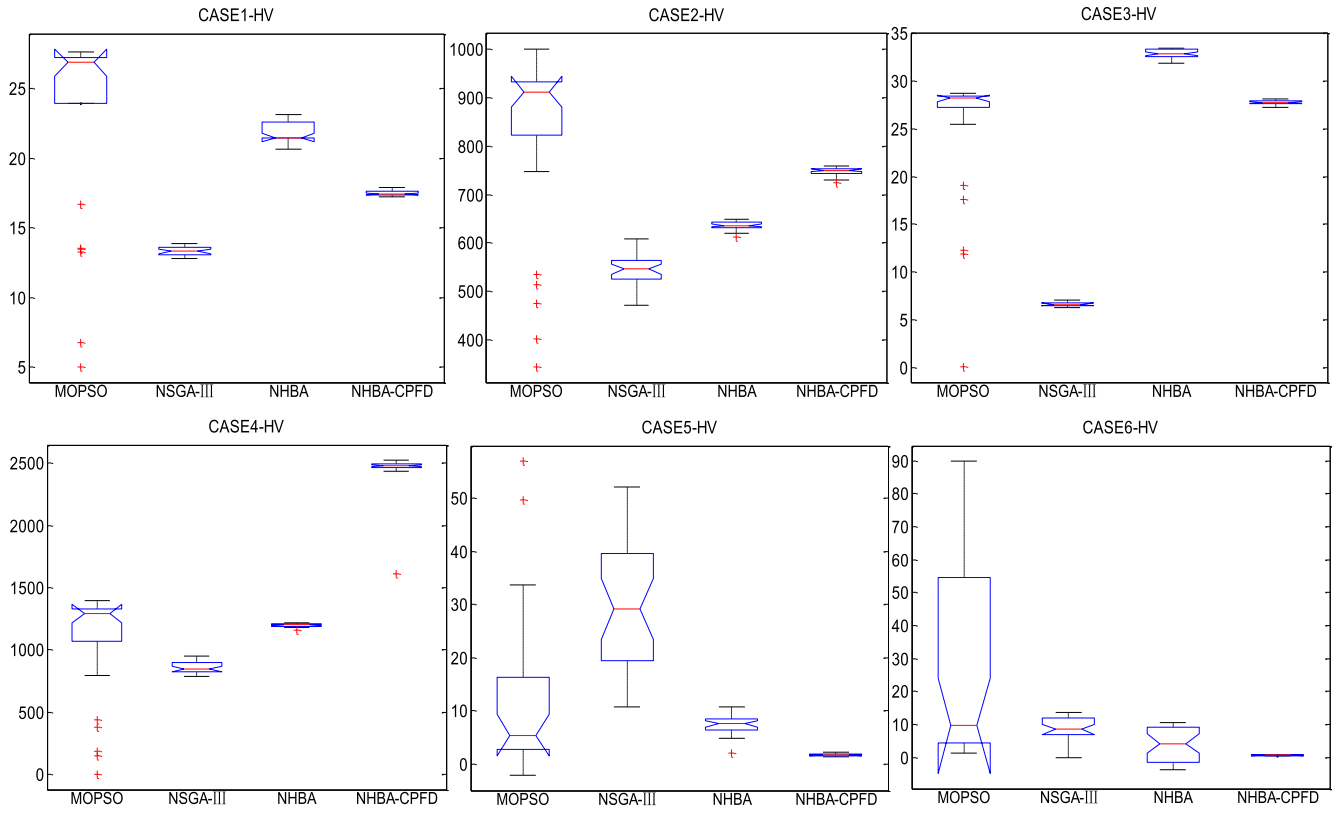

FIGURE 19. Boxplots of the HV index for *CASE1*∼*CASE6*.

TABLE 18. The mean and standard deviation of GD for CASE1∼CASE3.

GD	CASE1		CASE2		CASE3	
algorithm	mean	deviation	mean	deviation	mean	deviation
MOPSO	0.1479	0.0535	0.1471	0.0481	0.0990	0.0326
NSGA-III	0.0885	0.0203	0.1112	0.0249	0.0837	0.0191
NHBA	0.0815	0.0188	0.0798	0.0152	0.1222	0.0312
NHBA-CPFD	**0.0669**	**0.0128**	**0.0667**	**0.0127**	**0.0762**	**0.0146**

TABLE 19. The mean and standard deviation of GD for CASE4∼CASE6.

GD	CASE4		CASE5		CASE6	
algorithm	mean	deviation	mean	deviation	mean	deviation
MOPSO	0.0912	0.0217	0.0857	0.0195	0.4028	0.2146
NSGA-III	0.1820	0.0653	0.1310	0.0460	0.1032	0.0427
NHBA	0.0932	0.0226	0.0763	0.0148	0.0812	0.0239
NHBA-CPFD	**0.0744**	**0.0143**	**0.0725**	**0.0138**	**0.0637**	**0.0121**

TABLE 20. The mean and standard deviation of HV for CASE1∼CASE3.

HV	CASE1		CASE2		CASE3	
algorithm	mean	deviation	mean	deviation	mean	deviation
MOPSO	**23.2795**	6.7980	**829.3944**	181.2174	25.3801	6.6336
NSGA-III	13.3257	0.3111	545.7616	31.7056	6.6403	0.2127
NHBA	21.7154	0.8407	636.6639	**8.1124**	**32.7814**	0.4915
NHBA-CPFD	17.4836	**0.1606**	748.5426	8.1147	27.7229	**0.2293**

TABLE 21. The mean and standard deviation of HV for CASE4∼CASE6.

HV	CASE4		CASE5		CASE6	
algorithm	mean	deviation	mean	deviation	mean	deviation
MOPSO	1091.1038	414.2124	11.9814	15.4579	**25.0119**	27.6552
NSGA-III	858.4186	45.8371	**29.6216**	11.5932	8.6534	3.6423
NHBA	1199.2181	**11.8485**	7.3273	1.7977	3.7624	5.1423
NHBA-CPFD	**2448.6692**	159.3694	1.7520	**0.2630**	0.6430	**0.0779**

TABLE 22. The dominant relationship of BC solutions.

algorithm	The dominant relationship of obtained BCs										Ratio
	CASE1	CASE2	CASE3	CASE4	CASE5	CASE6	CASE7	CASE8	CASE9	CASE10	
MOPSO	Yes	Yes	Yes	Yes	U-R	Yes	Yes	Yes	Yes	U-R	80%
NSGA-III	Yes	Yes	U-R	Yes	U-R	Yes	Yes	Yes	U-R	U-R	60%
NHBA	Yes	U-R	U-R	Yes	U-R	U-R	Yes	Yes	Yes	Yes	60%

results of a bi-objective optimization problem (*CASE7*) on IEEE 57-node system and Figure 23 gives the results of a bi-objective optimization problem (*CASE9*) on IEEE 118-node system.

The superposition results also demonstrate that the convergence and extensive application of NHBA and NHBA-CPFD algorithms are clearly superior to that of MOPSO and NSGA-III algorithms. Especially, the proposed non-dominated sorting rule based on CPFD strategy is more potential to handle the MOOPF problems of large-scale complex systems.

E. COMPUTATIONAL COMPLEXITY

In the end, the average running time of 30 independent experiments, as a measure of computational complexity, is studied. The mean CPU time of four typical cases, which include three bi-objective cases on different scale systems and one tri-objective case on the IEEE 30-node system, is summarized in Table 23. It shows that compared with MOPSO and NSGA-III methods, the NHBA and NHBA-CPFD algorithms need more CPU time because of local searching process. It will be an important point for the further research on the improvement of bat algorithm.

TABLE 23. The mean CPU time.

algorithm	The mean CPU time (sec) with ite_{max}=500			
	CASE1	CASE5	CASE7	CASE9
MOPSO	190.79	298.84	472.50	2142.29
NSGA-III	189.61	302.12	453.75	2057.12
NHBA	207.07	317.38	511.41	2560.90
NHBA-CPFD	234.06	320.06	523.16	2504.91

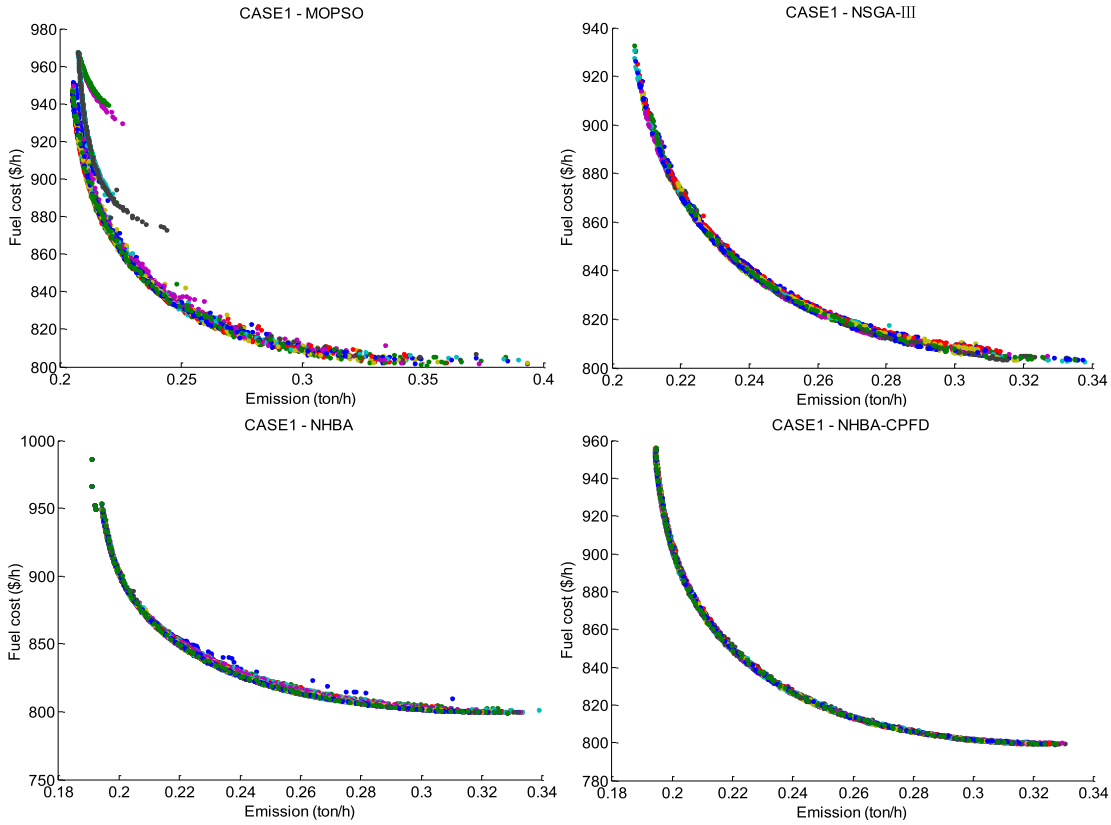

FIGURE 20. Results of 30 independent experiments for*CASE1*.

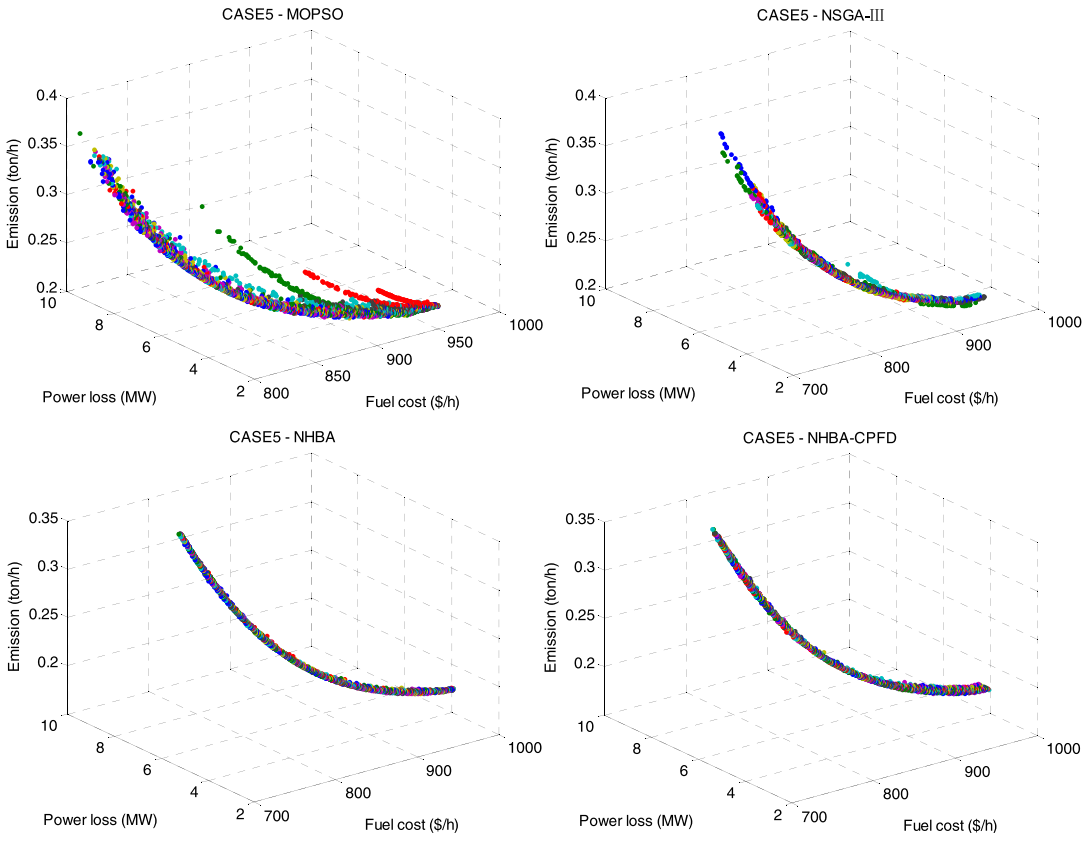

FIGURE 21. Results of 30 independent experiments for *CASE5*.

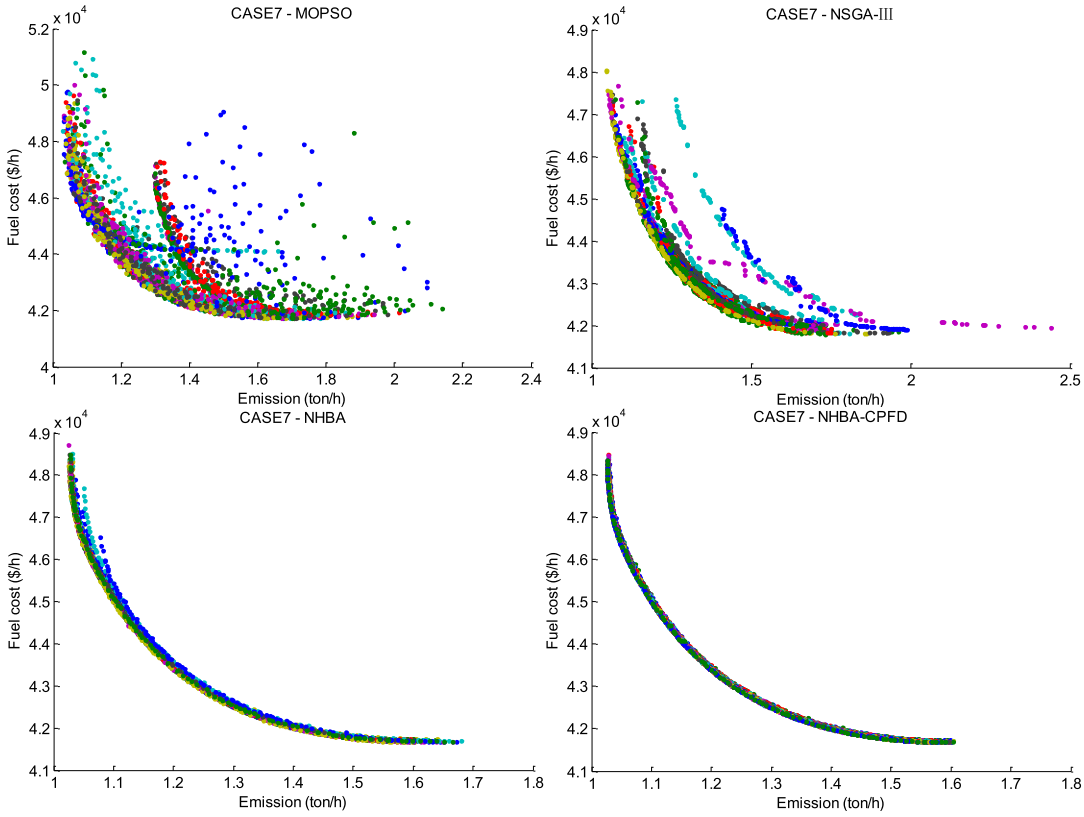

FIGURE 22. Results of 30 independent experiments for *CASE7*.

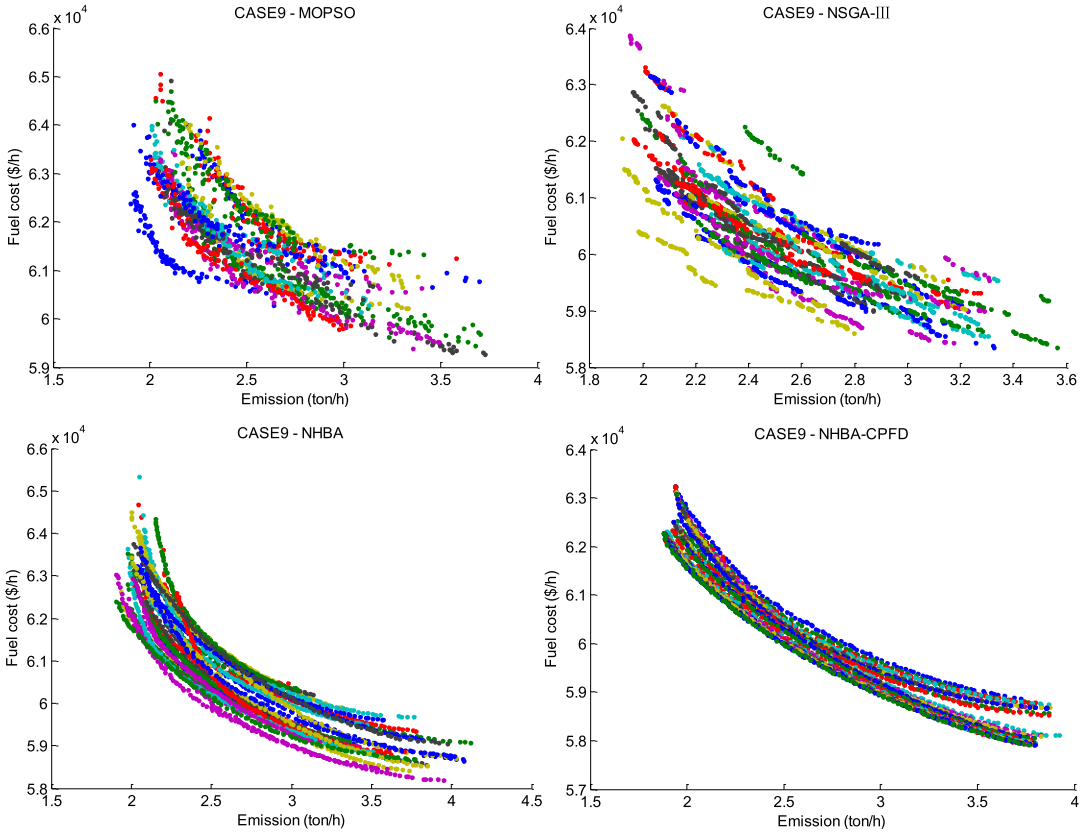

FIGURE 23. Results of 30 independent experiments for *CASE9*.

VII. CONCLUSION

The fast convergence and the optimal solution guiding mechanism of global bat algorithm make it suitable to solve the MOOPF problems. However, the original bat algorithm has the defect of being trapped in local optimum. A novel NHBA algorithm with nonlinear weight coefficient and MRFME model, enhanced by mutation and crossover mechanisms, is proposed to handle the strict-constrained MOOPF problems. Furthermore, a new non-dominated sorting method based on CPFD strategy is put forward to seek an evenly-distributed POS which can satisfy all restrictions of power system.

Ten multi-objective testing cases considering the fuel cost (with value-point loadings), the emission and the active power loss are carried out on the IEEE 30-node, IEEE 57-node and IEEE 118-node systems. Due to the complex-structure and high-dimension of large-scale power systems, the MOOPF problems on IEEE 57-node and IEEE 118-node systems have more computational difficulty. It should be exciting that, the simulation results of *CASE7*∼*CASE10* clearly indicate the presented NHBA-CPFD algorithm has superior performance in solving such MOOPF problems of complex electric system. The GD and HV indexes are utilized to measure the distribution and diversity of obtained POS. The evaluating results strongly demonstrate that the NHBA-CPFD algorithm is more desirable than the common-used MOPSO and NSGA-III algorithms, which is not only reflected in the preferable BC solutions, but also in the favorable-distribution and satisfactory-diversity of POS.

Therefore, the proposed NHBA-CPFD algorithm, which integrates the advantage of NHBA algorithm in determining high-quality BC solutions and the great edge of CPFD strategy in solving the higher-dimensional optimization problems of large-scale system, provides an innovative and effective way to deal with the MOOPF problems.

REFERENCES

[1] Y. Marinakis, M. Marinaki, and A. Migdalas, "A multi-adaptive particle swarm optimization for the vehicle routing problem with time windows," *Inf. Sci.*, vol. 481, pp. 311–329, May 2019.

[2] R. Chai, A. Savvaris, A. Tsourdos, S. Chai, Y. Xia, S. Wang, "Solving trajectory optimization problems in the presence of probabilistic constraints," *IEEE Trans. Cybern.*, to be published.

[3] A.-F. Attia, R. A. El Sehiemy, and H. M. Hasanien, "Optimal power flow solution in power systems using a novel Sine-Cosine algorithm," *Int. J. Elect. Power Energy Syst.*, vol. 99, pp. 331–343, Jul. 2018.

[4] L. Mackay, R. Guanotta, A. Dimou, G. Morales-España, L. Ramirez-Elizondo, and P. Bauer, "Optimal power flow for unbalanced bipolar DC distribution grids," *IEEE Access*, vol. 6, pp. 5199–5207, 2018.

[5] P. Chen, X. Xiao, and X. Wang, "Dynamic optimal power flow model incorporating interval uncertainty applied to distribution network," *IET Gener. Transmiss. Distrib.*, vol. 12, no. 12, pp. 2926–2936, Mar. 2018.

[6] G. Chen, L. Liu, Z. Zhang, and S. Huang, "Optimal reactive power dispatch by improved GSA-based algorithm with the novel strategies to handle constraints," *Appl. Soft Comput.*, vol. 50, pp. 58–70, Jan. 2017.

[7] D. Prasad, A. Mukherjee, G. Shankar, and V. Mukherjee, "Application of chaotic whale optimisation algorithm for transient stability constrained optimal power flow," *IET Sci. Meas. Technol.*, vol. 11, no. 8, pp. 1002–1013, Nov. 2017.

[8] G. Chen, S. Qiu, Z. Zhang, Z. Sun, and H. Liao, "Optimal power flow using gbest-guided cuckoo search algorithm with feedback control strategy and constraint domination rule," *Math. Problems Eng.*, vol. 2017, no. 2, pp. 1–14, Dec. 2017.

[9] S. Khunkitti, A. Siritaratiwat, S. Premrudeepreechacharn, R. Chatthaworn, and N. R. Watson, "A hybrid DA-PSO optimization algorithm for multi-objective optimal power flow problems," *Energies*, vol. 11, no. 9, p. 2270, Sep. 2018.

[10] S. Duman, "A modified moth swarm algorithm based on an arithmetic crossover for constrained optimization and optimal power flow problems," *IEEE Access*, vol. 6, pp. 45394–45416, 2018.

[11] J. B. Hmida, M. J. Morshed, J. Lee, and T. Chambers, "Hybrid imperialist competitive and grey wolf algorithm to solve multiobjective optimal power flow with wind and solar units," *Energies*, vol. 11, no. 11, p. 2891, Nov. 2018.

[12] Z. Liu, J. Yang, Y. Zhang, T. Ji, J. Zhou, and Z. Cai, "Multi-objective coordinated planning of active-reactive power resources for decentralized droop-controlled islanded microgrids based on probabilistic load flow," *IEEE Access*, vol. 6, pp. 40267–40280, 2018.

[13] X. Yuan *et al.*, "Multi-objective optimal power flow based on improved strength Pareto evolutionary algorithm," *Energy*, vol. 122, pp. 70–82, Mar. 2017.

[14] H. Liang, Y. Liu, F. Li, and Y. Shen, "A multiobjective hybrid bat algorithm for combined economic/emission dispatch," *Int. J. Elect. Power Energy Syst.*, vol. 101, pp. 103–115, Oct. 2018.

[15] X. Yuan, H. Tian, Y. Yuan, Y. Huang, and R. M. Ikram, "An extended NSGA-III for solution multi-objective hydro-thermal-wind scheduling considering wind power cost," *Energy Convers. Manage.*, vol. 96, pp. 568–578, May 2015.

[16] S. Sivasubramani and K. S. Swarup, "Multi-objective harmony search algorithm for optimal power flow problem," *Int. J. Electr. Power Energy Syst.*, vol. 33, no. 3, pp. 745–752, Mar. 2011.

[17] A. R. Bhowmik and A. K. Chakraborty, "Solution of optimal power flow using non dominated sorting multi objective opposition based gravitational search algorithm," *Int. J. Electr. Power Energy Syst.*, vol. 64, pp. 1237–1250, Jan. 2015.

[18] J. Zhang, Q. Tang, P. Li, D. Deng, and Y. Chen, "A modified MOEA/D approach to the solution of multi-objective optimal power flow problem," *Appl. Soft Comput.*, vol. 47, pp. 494–514, Oct. 2016.

[19] G. Chen, X. Yi, Z. Zhang, and H. Wang, "Applications of multi-objective dimension-based firefly algorithm to optimize the power losses, emission, and cost in power systems," *Appl. Soft Comput.*, vol. 68, pp. 322–342, Jul. 2018.

[20] X. Yang and A. H. Gandomi, "Bat algorithm: A novel approach for global engineering optimization," *Eng. Comput.*, vol. 29, nos. 5–6, pp. 464–483, 2012.

[21] M. A. Al-Betar, M. A. Awadallah, H. Faris, X.-S. Yang, A. T. Khader, and O. A. Alomari, "Bat-inspired algorithms with natural selection mechanisms for global optimization," *Neurocomputing*, vol. 273, pp. 448–465, Jan. 2018.

[22] E. Osaba, X. Yang, I. Fister, Jr., J. D. Ser, P. Lopez-Garcia, and A. J. Vazquez-Pardavila, "A discrete and improved bat algorithm for solving a medical goods distribution problem with pharmacological waste collection," *Swarm Evol. Comput.*, vol. 44, pp. 273–286, Feb. 2019.

[23] Y. Lu and T. Jiang, "Bi-population based discrete bat algorithm for the low-carbon job shop scheduling problem," *IEEE Access*, vol. 7, pp. 14513–14522, 2019.

[24] G. Chen, L. Liu, P. Song, and Y. Du, "Chaotic improved PSO-based multi-objective optimization for minimization of power losses and L index in power systems," *Energy Convers. Manage.*, vol. 86, pp. 548–560, Oct. 2014.

[25] G. Chen, X. Yi, Z. Zhang, and H. Lei, "Solving the multi-objective optimal power flow problem using the multi-objective firefly algorithm with a constraints-prior pareto-domination approach," *Energies*, vol. 11, no. 12, no. 3438, Dec. 2018.

[26] W. Warid, H. Hizam, N. Mariun, and N. I. A. Wahab, "A novel quasi-oppositional modified Jaya algorithm for multi-objective optimal power flow solution," *Appl. Soft Comput.*, vol. 65, pp. 360–373, Apr. 2018.

[27] G. Chen, Z. Lu, and Z. Zhang, "Improved krill herd algorithm with novel constraint handling method for solving optimal power flow problems," *Energies*, vol. 11, no. 761, Jan. 2018.

[28] S. Huang and V. Dinavahi, "Fast batched solution for real-time optimal power flow with penetration of renewable energy," *IEEE Access*, vol. 6, pp. 13898–13910, 2018.

[29] S. Dhar and M. K. Kundu, "A novel method for image thresholding using interval type-2 fuzzy set and Bat algorithm," *Appl. Soft Comput.*, vol. 63, pp. 154–166, Feb. 2018.
[30] R. Murugan, M. R. Mohan, C. C. A. Rajan, P. D. Sundari, and S. Arunachalam, "Hybridizing bat algorithm with artificial bee colony for combined heat and power economic dispatch," *Appl. Soft Comput.*, vol. 72, pp. 189–217, Nov. 2018.
[31] J. Zhang, S. Chen, R. Zhang, A. F. Al Rawi, and L. Hanzo, "Differential evolution algorithm aided turbo channel estimation and multi-user detection for G.Fast systems in the presence of FEXT," *IEEE Access*, vol. 6, pp. 33111–33128, 2018.
[32] R. Chai, A. Savvaris, A. Tsourdos, and S. Chai, "Multi-objective trajectory optimization of space manoeuvre vehicle using adaptive differential evolution and modified game theory," *Acta Astronautica*, vol. 136, pp. 273–280, Jul. 2017.
[33] L. Lin and M. Zhu, "Efficient tracking of moving target based on an improved fast differential evolution algorithm," *IEEE Access*, vol. 6, pp. 6820–6828, 2018.
[34] R. Chai *et al.*, "Unified multiobjective optimization scheme for aeroassisted vehicle trajectory planning," *J. Guid., Control Dyn.*, vol. 41, no. 7, pp. 1521–1530, 2018.
[35] K. Deb, A. Pratap, S. Agarwal, and T. Meyarivan, "A fast and elitist multiobjective genetic algorithm: NSGA-II," *IEEE Trans. Evol. Comput.*, vol. 6, no. 2, pp. 182–197, Apr. 2002.
[36] P. C. Roy, K. Deb, and M. M. Islam, "An efficient nondominated sorting algorithm for large number of fronts," *IEEE Trans. Cybern.*, vol. 49, no. 3, pp. 859–869, Mar. 2019.
[37] A.-A. A. Mohamed, Y. S. Mohamed, A. A. M. El-Gaafary, and A. M. Hemeida, "Optimal power flow using moth swarm algorithm," *Electr. Power Syst. Res.*, vol. 142, pp. 190–206, Jan. 2017.
[38] A. E. Chaib, H. R. E. H. Bouchekara, R. Mehasni, and M. A. Abido, "Optimal power flow with emission and non-smooth cost functions using backtracking search optimization algorithm," *Int. J. Elect. Power Energy Syst.*, vol. 81, pp. 64–77, Oct. 2016.
[39] H. Pulluri, R. Naresh, and V. Sharma, "An enhanced self-adaptive differential evolution based solution methodology for multiobjective optimal power flow," *Appl. Soft Comput.*, vol. 54, pp. 229–245, May 2017.
[40] M. Ghasemi, S. Ghavidel, M. M. Ghanbarian, and M. Gitizadeh, "Multi-objective optimal electric power planning in the power system using Gaussian bare-bones imperialist competitive algorithm," *Inf. Sci.*, vol. 294, pp. 286–304, Feb. 2015.
[41] N. Daryani, M. T. Hagh, and S. Teimourzadeh, "Adaptive group search optimization algorithm for multi-objective optimal power flow problem," *Appl. Soft Comput.*, vol. 38, pp. 1012–1024, Jan. 2016.
[42] H. Ishibuchi, H. Masuda, Y. Tanigaki, and Y. Nojima, *Modified Distance Calculation in Generational Distance and Inverted Generational Distance* (Lecture Notes in Computer Science), vol. 9019 A. GasparCunha, C. H. Antunes, and C. C. Coello, Eds. Cham, Switzerland: Springer, 2015, pp. 110–125.
[43] H. Ishibuchi, R. Imada, Y. Setoguchi, and Y. Nojima, "Reference point specification in inverted generational distance for triangular linear Pareto front," *IEEE Trans. Evol. Comput.*, vol. 22, no. 6, pp. 961–975, Dec. 2018.

GONGGUI CHEN received the B.S. degree in physics from Huazhong Normal University, the M.E. degree in computer technology and the Ph.D. degree in electrical engineering from the Huazhong University of Science and Technology (HUST), China. He is currently a Professor with the Department of Electrical Engineering, College of Automation, Chongqing University of Posts and Telecommunications, Chongqing, China. His research interests include economic dispatch, optimal power flow, and application of artificial intelligence in power systems.

JIE QIAN received the bachelor's degree in electrical engineering and automation from the Chongqing University of Posts and Telecommunications (CQUPT), Chongqing, China, in 2017, where she is currently pursuing the master's degree. Her research interests include optimal power flow and application of artificial intelligence in power systems.

ZHIZHONG ZHANG received the M.S. degree in communication network testing from the Chongqing University of Posts and Telecommunications, China, in 1998, and the Ph.D. degree from the School of Communication Engineering, University of Electronic Science and Technology of China, in 2002. He is currently a Professor with the Chongqing University of Posts and Telecommunications. His research interests include mobile communication testing technology, broadband information networking, 5G networking, and optimal power flow in power systems.

ZHI SUN received the B.E. degree in computer science and technology and the M.E. degree in electrical engineering from the Huazhong University of Science and Technology (HUST), in 2004 and 2012, respectively. He is currently an Electronic Engineer with Chn Energy Enshi Hydropower Co., Ltd., China. His research interests include intelligent substation, economic dispatch, optimal power flow, and application of artificial intelligence in power systems.